Observations of radiocarbon in CO_2 at La Jolla, California, USA 1992–2007: Analysis of the long-term trend

Heather D. Graven,[1,2] Thomas P. Guilderson,[3,4] and Ralph F. Keeling[1]

Received 11 July 2011; revised 9 November 2011; accepted 16 November 2011; published 25 January 2012.

[1] High precision measurements of $\Delta^{14}C$ were performed on CO_2 sampled at La Jolla, California, USA over 1992–2007. A decreasing trend in $\Delta^{14}C$ was observed, which averaged -5.5 ‰ yr^{-1} yet showed significant interannual variability. Contributions to the trend in global tropospheric $\Delta^{14}C$ by exchanges with the ocean, terrestrial biosphere and stratosphere, by natural and anthropogenic ^{14}C production and by ^{14}C-free fossil fuel CO_2 emissions were estimated using simple models. Dilution by fossil fuel emissions made the strongest contribution to the $\Delta^{14}C$ trend while oceanic ^{14}C uptake showed the most significant change between 1992 and 2007, weakening by 70%. Relatively steady positive influences from the stratosphere, terrestrial biosphere and ^{14}C production moderated the decreasing trend. The most prominent excursion from the average trend occurred when $\Delta^{14}C$ decreased rapidly in 2000. The rapid decline in $\Delta^{14}C$ was concurrent with a rapid decline in atmospheric O_2, suggesting a possible cause may be the anomalous ventilation of deep ^{14}C-poor water in the North Pacific Ocean. We additionally find the presence of a 28-month period of oscillation in the $\Delta^{14}C$ record at La Jolla.

Citation: Graven, H. D., T. P. Guilderson, and R. F. Keeling (2012), Observations of radiocarbon in CO_2 at La Jolla, California, USA 1992–2007: Analysis of the long-term trend, *J. Geophys. Res.*, *117*, D02302, doi:10.1029/2011JD016533.

1. Introduction

[2] Long term atmospheric measurements of radiocarbon, ^{14}C, in CO_2 began in 1954 at Wellington, New Zealand [*Rafter*, 1955]. Since then, observations from New Zealand [*Rafter and Fergusson*, 1957; *Manning et al.*,1990; *Currie et al.*, 2009], Norway [*Nydal and Lövseth*, 1965, 1983], central Europe [*Levin et al.*, 1985; *Levin and Kromer*, 2004] and other sites have recorded large changes in the $^{14}C/C$ ratio of CO_2. In the 1950s and 1960s, testing of nuclear weapons added an excess of ^{14}C atoms that approximately doubled the atmospheric inventory of ^{14}C. As the testing ceased and bomb-derived ^{14}C entered the oceanic and terrestrial carbon reservoirs, observations of $^{14}C/C$ in CO_2 revealed a quasi-exponential decline that enabled investigation of mixing rates between different parts of the atmosphere and exchange rates between the atmosphere and the ocean and terrestrial ecosystems [e.g., *Rafter and Fergusson*, 1957; *Lal and Rama*, 1966; *Goudriaan*, 1992; *Hesshaimer et al.*, 1994; *Trumbore*, 2000; *Naegler et al.*, 2006].

[3] Presently, ^{14}C exchanges between the atmosphere and the ocean and terrestrial biosphere are redistributing the bomb-derived excess ^{14}C from short term to longer term reservoirs. ^{14}C exchanges are also responding to the dilution of atmospheric ^{14}C by fossil fuel-derived CO_2 which has no ^{14}C because of radioactive decay [*Suess*, 1955; *Keeling*, 1979; *Tans et al.*, 1979; *Stuiver and Quay*, 1981]. Since the response of land and ocean carbon reservoirs to these perturbations in $^{14}C/C$ is governed by the same exchange processes that determine anthropogenic CO_2 uptake and storage, continued observation and understanding of ^{14}C dynamics can provide constraints on terrestrial and oceanic carbon cycling and the potential magnitude and sustainability of CO_2 sinks [*Levin and Hesshaimer*, 2000; *Randerson et al.*, 2002].

[4] $^{14}C/C$ ratios can also be used to identify local additions of CO_2 from fossil fuel emissions by observation of ^{14}C dilution in comparison to background air [e.g., *Tans et al.*, 1979; *Levin et al.*, 1989; *Meijer et al.*, 1996; *Turnbull et al.*, 2006; *Levin and Rödenbeck*, 2008]. Quantification of fossil fuel-derived CO_2 can be useful for resolving budgets of CO_2 contributions from industrial versus biospheric or oceanic sources [e.g., *Turnbull et al.*, 2006; *Graven et al.*, 2009], for detecting temporal or spatial patterns in fluxes of different types [e.g., *Hsueh et al.*, 2007; *Turnbull et al.*, 2009a], or for estimating fossil fuel emissions within a catchment area [e.g., *Levin et al.*, 2003; *van der Laan et al.*, 2010; *Turnbull et al.*, 2011]. The use of atmospheric observations to estimate fossil fuel emissions promises to become important as emissions of CO_2 and other greenhouse gases are more heavily regulated and require independent verification of economic data-based

[1]Scripps Institution of Oceanography, University of California, San Diego, La Jolla, California, USA.
[2]Institute of Biogeochemistry and Pollutant Dynamics, ETH Zurich, Zurich, Switzerland.
[3]Center for Accelerator Mass Spectrometry, Lawrence Livermore National Laboratory, Livermore, California, USA.
[4]Department of Ocean Sciences, University of California, Santa Cruz, California, USA.

Copyright 2012 by the American Geophysical Union.
0148-0227/12/2011JD016533

inventories [*Nisbet*, 2005; *Marquis and Tans*, 2008]. Measurements that resolve variability in background air are essential to this technique since uncertainty in background air composition limits the precision of observation-based estimates of fossil fuel-derived CO_2 [*Graven et al.*, 2009; *Turnbull et al.*, 2009b].

[5] Measurements of $^{14}C/C$ ratios are typically referenced to the Modern Standard and reported as $\Delta^{14}C$, which includes a correction for radioactive decay between sampling and analysis and a correction for mass-dependent fractionation using measurements of $^{13}C/^{12}C$ in the sample [*Stuiver and Polach*, 1977]. Use of $\Delta^{14}C$ notation eliminates the effect of fractionating processes such as photosynthetic assimilation or oceanic CO_2 uptake on the $^{14}C/C$ ratio in CO_2. $\Delta^{14}C$ in CO_2 is therefore sensitive to natural and anthropogenic ^{14}C production as well as to exchanges of carbon with reservoirs that have a different $\Delta^{14}C$ signature.

[6] Here we present $\Delta^{14}C$ measurements in CO_2 samples from La Jolla, California, USA collected at roughly monthly intervals between 1992 and 2007. In this paper, we focus on analyzing the $\Delta^{14}C$ trend over the 16-year record. We compare the observed trend to simple models of the contributions to the global tropospheric trend in $\Delta^{14}C$ between 1992 and 2007 from the release of fossil fuel CO_2, natural and anthropogenic production of ^{14}C and carbon exchanges with the stratosphere, ocean, and biosphere. We then evaluate interannual variability in the trend of $\Delta^{14}C$. In the accompanying paper, we present $\Delta^{14}C$ observations from 6 other global sites for 2- to 9-year periods ending in 2007 and examine spatial gradients and seasonal cycles [*Graven et al.*, 2012].

2. Methods

[7] Atmospheric flask sampling at La Jolla, California is conducted at the Scripps Pier (32.87°N, 117.25°W) when meteorological conditions are favorable for collecting clean, marine air and avoiding local contamination. Such conditions are met when strong, stable winds originating from the southwesterly sector (offshore) are present and a low, stable CO_2 concentration is identified with a continuous CO_2 analyzer.

[8] The representativeness of air collected at La Jolla under clean air conditions can be assessed by comparing observed CO_2 concentrations with other background sites. Observed annual mean CO_2 gradients are less than ± 0.2 ppm between La Jolla and the Pacific Ocean Station at 30°N, 122.85°W [*Conway and Tans*, 2004] and less than ± 0.5 ppm between La Jolla and other Scripps CO_2 stations in closest proximity (Kumukahi, Hawaii and Point Barrow, Alaska) [*Keeling and Piper*, 2001; *Keeling et al.*, 2011]. The CO_2 concentration in the air collected at La Jolla is slightly higher than Kumukahi and slightly lower than Point Barrow, in accordance with the observed meridional CO_2 gradient in background air [*Keeling and Piper*, 2001; *Masarie and Tans*, 1995; *Keeling et al.*, 2011]. The seasonal cycle of $\Delta^{14}C$ at La Jolla, presented in the accompanying paper, also supports the representativeness of clean, marine air sampled under these conditions. If local contamination strongly contributed to the seasonal cycle of $\Delta^{14}C$ at La Jolla, the minimum in $\Delta^{14}C$ would be expected to occur in the fall months when polluted continental air is transported offshore most frequently [*Conil and Hall*, 2006; *Riley et al.*, 2008]. In fact, the maximum $\Delta^{14}C$ occurs in the fall months at La Jolla, consistent with other Northern Hemisphere observations of background air [*Graven et al.*, 2012; *Levin and Kromer*, 2004; *Turnbull et al.*, 2007].

[9] Evacuated 5 L spherical glass flasks are sampled by opening a single ground taper joint stopcock sealed with Apiezon® grease and filling with whole air. At La Jolla, six flasks are sampled concurrently, while at other Scripps CO_2 stations, 2–3 flasks are sampled concurrently. Flask air is dried and the CO_2 concentration is measured by non-dispersive infrared gas analysis [*Keeling et al.*, 2002] at the Scripps laboratory. CO_2 is extracted from the remaining flask air by passing 2–4 L of air through a spiral quartz trap immersed in liquid nitrogen, then the CO_2 sample is sealed and stored in a Pyrex® tube. The same flask handling, storage and extraction procedures are used for analysis of $\delta^{13}C$ in CO_2 at Scripps with measurement precision of <0.03 ‰ [*Guenther et al.*, 2001]. An archive of such CO_2 samples dating back to July 1992 from La Jolla was available for analysis. Samples collected between July 1992 and December 2007 were analyzed for ^{14}C in CO_2, including 79 sample dates for which two or more replicate samples were measured. These CO_2 samples were analyzed together with CO_2 samples from six other sites [*Graven et al.*, 2012].

[10] All CO_2 samples were converted to graphite and analyzed by accelerator mass spectrometry (AMS) at the Center for Accelerator Mass Spectrometry at Lawrence Livermore National Laboratory (LLNL) between 2003 and 2009 [*Graven et al.*, 2007; *Graven*, 2008]. We utilize the $\Delta^{14}C$ notation implicitly as a geochemical sample with known age and $\delta^{13}C$ correction (equivalent to Δ in work by *Stuiver and Polach* [1977]). Ratios of $^{14}C/C$ are corrected for decay between sampling and analysis dates and for mass dependent fractionation using $\delta^{13}C$. The $\delta^{13}C$ correction uses $\delta^{13}C$ measured in concurrently sampled CO_2 [*Guenther et al.*, 2001] to normalize atmospheric samples to the -25 ‰ reference. Unlike some smaller AMS systems which cause significant fractionation during ionization, there is no evidence for fractionation within the LLNL AMS ion source [*Proctor et al.*, 1990]. This is shown by nearly constant $^{14}C/^{13}C$ ratios measured throughout the analysis of individual samples [*Fallon et al.*, 2007]. Slight drifts in $^{14}C/^{13}C$ ratios can be attributed to stripping efficiency and are successfully canceled by normalization with reference materials. Therefore, in-line $\delta^{13}C$ correction is not required or performed at LLNL.

[11] Individual measurement uncertainty in $\Delta^{14}C$ is ± 1.7 ‰ for most samples, where uncertainty is determined by the reproducibility of $\Delta^{14}C$ in CO_2 extracted from whole air reference cylinders [*Graven et al.*, 2007; *Graven*, 2008]. Measurements conducted prior to 2006 have uncertainties between ± 1.7 and ± 3.3 ‰ [*Graven*, 2008], since sample handling and data processing were not yet optimized for CO_2 samples. However, drawing on a large archive of existing samples allowed the samples to be selected randomly for analysis between 2003 and 2009. Samples from different years and different sites were included in each measurement batch [*Graven*, 2008], so that differences in uncertainty between measurement batches can be expected

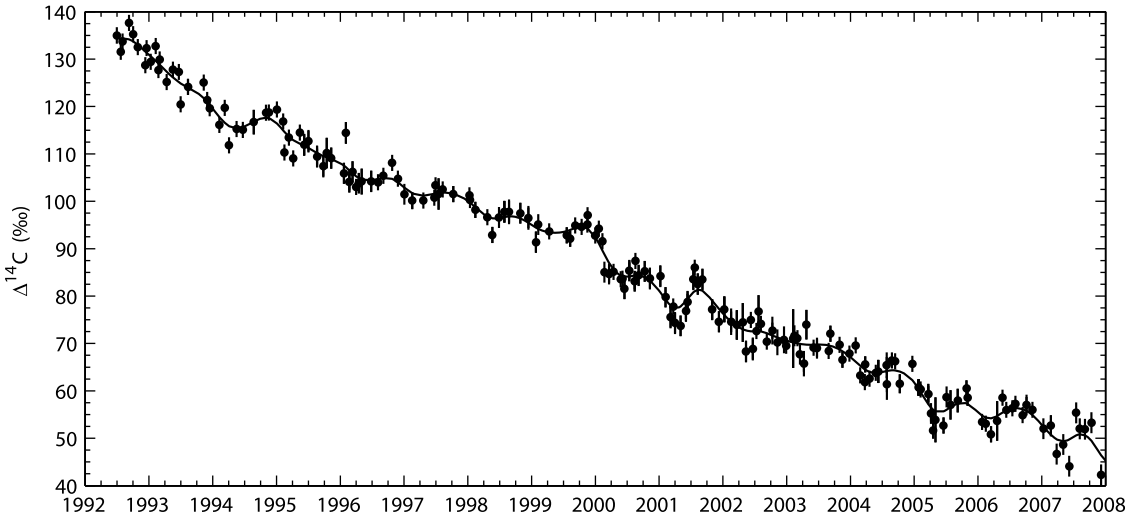

Figure 1. $\Delta^{14}C$ measured in CO_2 sampled at La Jolla with a cubic smoothing spline. Replicate measurements have been averaged. Error bars show measurement uncertainty or the standard deviation in $\Delta^{14}C$ of replicate samples, whichever is larger.

to have little impact on the features contained in the atmospheric records.

3. $\Delta^{14}C$ Observations

[12] Measurements of $\Delta^{14}C$ are shown in Figure 1 and listed in Appendix A. These data are also available at the Scripps CO_2 Program Web site: http://scrippsco2.ucsd.edu/.

[13] Figure 2a shows seasonally adjusted observations of $\Delta^{14}C$ at La Jolla to emphasize variations in the data that occur at timescales longer than one year. Seasonal cycles are presented and discussed in the accompanying paper [*Graven et al.*, 2012]. The seasonal cycles were removed by first detrending the data with a cubic smoothing spline with cutoff period of 24 months [*Enting*, 1987]. Second, a loose cubic smoothing spline was fit to the detrended data (cutoff period of 4 months) and finally, the loose spline was subtracted from the original observations.

[14] $\Delta^{14}C$ at La Jolla decreased by nearly 100 ‰ between 1992 and 2007. A linear least squares fit to all measurements results in a slope of -5.5 ± 0.1 ‰ yr^{-1}, where 0.1 is the 1-σ uncertainty [*Cantrell*, 2008]. The trend was slightly weaker during the second half of the observation period; a linear fit to observations between mid-2001 and the end of 2007 yields a slope of -5.0 ± 0.2 ‰ yr^{-1} [*Graven et al.*, 2012] while a fit to observations between mid-1992 to mid-2001 yields -5.7 ± 0.1 ‰ yr^{-1}. We have also fit an exponential trend to the observed $\Delta^{14}C$; the derivative of the exponential and linear fits are shown in Figure 2b. Compared to the constant trend of -5.5 ‰ yr^{-1} computed by the linear fit, the exponential derivative slows from -8 ‰ yr^{-1} in 1992 to -3 ‰ yr^{-1} in 2007.

[15] Figure 2b also shows the derivative of the seasonally adjusted $\Delta^{14}C$ observations. The growth rate of $\Delta^{14}C$ at La Jolla showed large variability over 1992–2007. The strongest excursion from the linear or exponential trend was an especially rapid decrease in $\Delta^{14}C$ in 2000. Local minima in the trend of $\Delta^{14}C$ are also observed at roughly 2 year intervals, suggesting a short term periodicity exists in $\Delta^{14}C$ at La Jolla. Features of variability in the trend are not likely to be artifacts of the spline fitting technique, since trends calculated using annual means (Section 5.2) and low-pass filtering (Section 5.3) show similar features.

4. Global Trend in Tropospheric $\Delta^{14}C$

4.1. Description of Box Model Formulation

[16] In this section, we will describe the box model formulation used to simulate influences on the trend in $\Delta^{14}C$

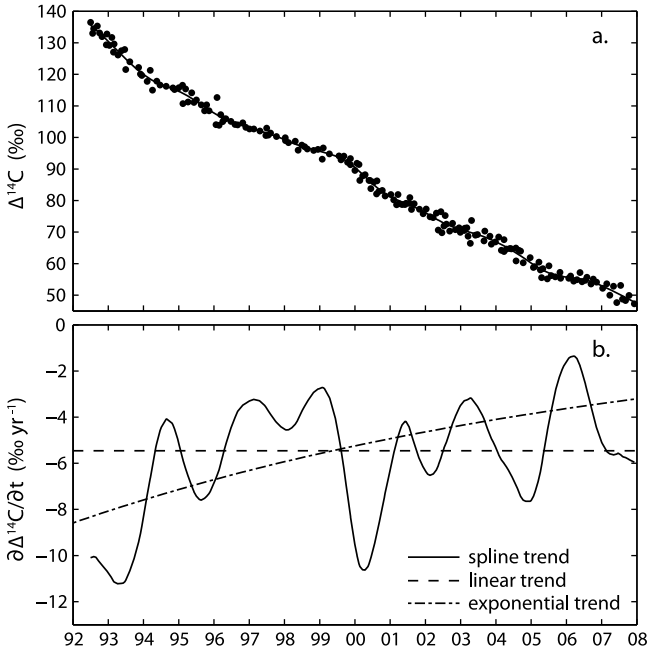

Figure 2. (a) Seasonally adjusted $\Delta^{14}C$ at La Jolla with a cubic smoothing spline. (b) The derivative of the spline curve from Figure 2a is shown as the solid line. Also shown in Figure 2b are lines representing the derivative of a linear fit (dashed, -5.5 ‰ yr^{-1}) and an exponential fit (dash-dotted).

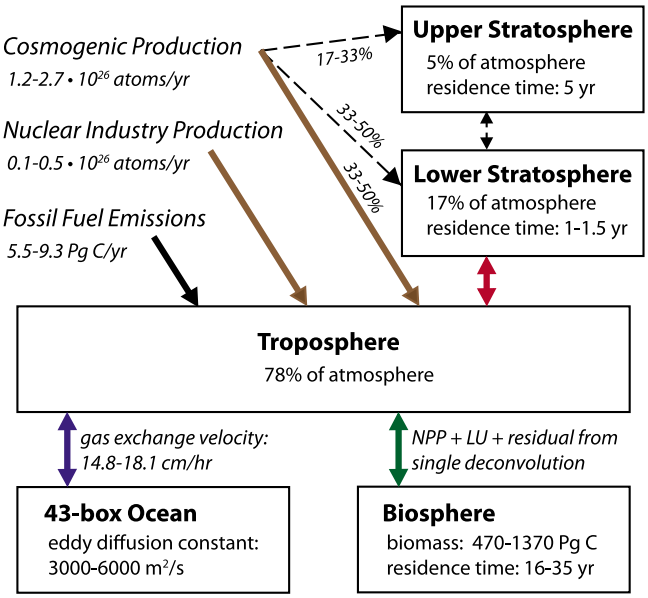

Figure 3. Schematic of the box model setup and parameter values used to estimate contributions to the global tropospheric $\Delta^{14}C$ trend. Colored lines indicate carbon and isotopic fluxes that correspond to the individual contributions plotted in Figure 4; dashed lines indicate fluxes to stratospheric reservoirs that affect the troposphere indirectly.

from the emission of fossil fuel-derived ^{14}C-free CO_2, natural and anthropogenic ^{14}C production, and ^{14}C and carbon exchanges between the troposphere and the ocean, the land biosphere, and the stratosphere. In Section 4.2, we will present the results of the model and in Section 5.1, we will discuss the results, the limitations of the simple models used here, and a comparison with similar calculations performed by *Levin et al.* [2010].

[17] The influence on tropospheric $\Delta^{14}C$ from exchange with a carbon reservoir is primarily determined by the $\Delta^{14}C$ disequilibrium. In order to formulate the most precise estimate of these influences, we used the observed tropospheric $\Delta^{14}C$, $\delta^{13}C$ and CO_2 to calculate the evolution of $\Delta^{14}C$ and carbon and isotopic fluxes in separate, uncoupled forward models of the ocean, biosphere and stratosphere. We then synthesize the separate model contributions and evaluate the correspondence between the simulated and observed $\Delta^{14}C$ trend. While individual components are forced by observed atmospheric changes, they are not constrained to add up to the observed overall $\Delta^{14}C$ change in the atmosphere. A comparison of the sum of the components with observations thus provides an important consistency check. Estimates of global averages were formulated by weighted averages of clean-air station data including results from *Neftel et al.* [1994] and *Keeling and Whorf* [2005] for atmospheric CO_2 concentrations, from *Friedli et al.* [1986] and *Keeling et al.* [2005] for $\delta^{13}C$, and from this work and that of *Stuiver et al.* [1998], *Levin and Kromer* [2004], *Levin et al.* [2007] and *Graven et al.* [2012] for $\Delta^{14}C$.

[18] The box model setup is depicted in Figure 3 and summarized in Table 1. The biospheric and oceanic components were initialized with simulations of constant preindustrial atmospheric composition lasting 30,000 years to achieve steady state. Then, simulations of the biospheric and oceanic components were conducted using records of atmospheric composition beginning in 1511 for $\Delta^{14}C$ [*Stuiver et al.*, 1998] and 1720 and 1744 for CO_2 concentrations and $\delta^{13}C$ [*Neftel et al.*, 1994; *Friedli et al.*, 1986], respectively. The stratospheric component was simulated beginning in 1900. We present model results for the period of observation at La Jolla: 1992 through the end of 2007.

[19] The decrease in $\Delta^{14}C$ caused by fossil fuel emissions was estimated by mixing the global annual CO_2 emissions from inventories of economic data [*Marland et al.*, 2008; *Canadell et al.*, 2007] into the entire troposphere (78% of the atmosphere). We included a 10% uncertainty in reported emissions, slightly larger than estimates of 8% by *Andres et al.* [1996] and 5% by *Canadell et al.* [2007].

[20] Air-sea exchange was estimated by several simulations of a 43-box diffusion model including CO_2 and ^{14}C and ^{13}C isotopes [*Oeschger et al.*, 1975], using a piston velocity of 14.8 to 18.1 cm hr^{-1} and an eddy diffusion coefficient of 3000 to 6000 m^2 yr^{-1}. The specification of piston velocity uses results from previous studies that constrained the globally averaged piston velocity with observations of the oceanic inventory of bomb-derived ^{14}C [*Sweeney et al.*, 2007; *Naegler et al.*, 2006] and oceanic $\Delta^{14}C$ and $\delta^{13}C$ distributions [*Krakauer et al.*, 2006]. We selected three values across the range in piston velocity (14.8, 16.3 and 18.1 cm hr^{-1}). Then we selected eddy diffusion coefficients that allowed the simulated average oceanic depth profile of natural ^{14}C [*Oeschger et al.*, 1975] and the simulated oceanic inventory of anthropogenic CO_2 [*Sabine et al.*, 2004] to roughly match observations, in addition to allowing the simulated total bomb-derived ^{14}C in our modeled carbon system (including the atmosphere and terrestrial biosphere, see below) to be consistent with *Naegler and Levin* [2006]. We used four values for the eddy diffusion coefficient (3000, 4000, 5000 and 6000 m^2 yr^{-1}), which are specific to our model setup. One combination of piston velocity and eddy diffusion coefficient (18.1 cm hr^{-1} and 6000 m^2 yr^{-1}) did not fit our constraints, so this pair of parameter values was excluded.

[21] Terrestrial ecosystem exchange was estimated by several simulations of a one-box model of the biosphere. The biosphere was assigned a total preindustrial amount of overturning biomass of 470 to 1370 Pg C and a CO_2 fertilization factor [*Keeling et al.*, 1989] of 0 to 0.4, with global net primary production (NPP) of 24 to 42 Pg C yr^{-1} and average ecosystem residence time of 16 to 35 years between 1992–2007. Sets of parameter values were chosen to match a total bomb-derived ^{14}C excess of $615 \cdot 10^{26}$ atoms [*Naegler and Levin*, 2006], including the atmospheric inventory and the ocean inventory from simulations of our one-dimensional model (see above). We allowed a range in total bomb-derived ^{14}C of $\pm 35 \cdot 10^{26}$ atoms, twice as large as the uncertainty reported by *Naegler and Levin* [2006]. We neglect the fraction of NPP for which the assimilated carbon is returned to the atmosphere within 1–3 years, one-third or more of NPP [*Randerson et al.*, 2006], since the respiration of such

young carbon does not substantially affect tropospheric $\Delta^{14}C$ over 1992–2007 (less than 0.4 ‰ yr^{-1}). Allowing for the fraction of NPP and biomass that are neglected by this assumption, the total biospheric mass and NPP in our simple model (470–1370 Pg C and 24–42 Pg C yr^{-1}) are similar to current dynamic global vegetation models [*Cramer et al.*, 2001; *Friedlingstein et al.*, 2006]. Additional annual carbon, ^{13}C and ^{14}C fluxes to or from the biosphere were assigned based on the land use (LU) flux of *Houghton* [2008] and the residual fluxes from a single deconvolution between the fossil fuel and land use sources, the observed atmospheric CO_2 growth and the box diffusion model representation of oceanic CO_2 uptake [*Siegenthaler and Oeschger*, 1987].

[22] Cosmogenic production was simulated to occur at an average rate of $2.16 \cdot 10^{26}$ atoms yr^{-1}, which is 35–40% lower than the rate estimated by *Lal* [1992] and *Masarik and Beer* [2009]. The total production rate was reduced from *Lal* [1992] and *Masarik and Beer* [2009] in order to match the pre-bomb global ^{14}C inventory simulated by our oceanic and biospheric models. Observations of ^{14}CO [*Manning et al.*, 2005] support a higher cosmogenic production rate, similar to that predicted by *Lal* [1992] and *Masarik and Beer* [2009]. However, as in work by *Levin et al.* [2010], the use of a smaller average production rate was necessary to achieve a steady state in our modeled carbon system. Modulation of ^{14}C production by the sunspot cycle was included according to observations of the cosmic neutron flux at Climax, Colorado, USA (available at http://ulysses.sr.unh.edu/NeutronMonitor/neutron_mon.html), using relationships between the cosmic neutron flux and the solar modulation parameter from *Lal* [1992], *Masarik and Beer* [1999] and *Lowe and Allan* [2002]. Simulated production varied by ±15% [*Lal*, 1992; *Masarik and Beer*, 1999] over the sunspot cycle and an uncertainty of ±10% in the total production rate was included. One-half to two-thirds of cosmogenic ^{14}C production was prescribed to occur in the stratosphere, with the rest occurring in the troposphere [*O'Brien*, 1979; *Jöckel et al.*, 1999].

[23] Production of ^{14}C by nuclear power plants was calculated using energy statistics and emission factors of ^{14}C release per unit electrical power generation for 6 different reactor types [*United Nations Scientific Committee on the Effects of Atomic Radiation* (*UNSCEAR*), 2000; *Graven and Gruber*, 2011]. Electrical output from each type of reactor was gathered from the International Atomic Energy Agency's Power Reactor Information System (available at http://www.iaea.org/programmes/a2/). We also accounted for ^{14}C released by 4 spent nuclear fuel reprocessing facilities where ^{14}C emission data was available [*UNSCEAR*, 2000; *Schneider and Marignac*, 2008; *Nakada et al.*, 2008; *UK Environmental Agency*, 2008; *Anzai et al.*, 2008], which amounted to 7–16% of the release from nuclear power plants. Total ^{14}C production from the nuclear energy industry was $0.28 \cdot 10^{26}$ atoms in 1992, which was 13% of the rate of cosmogenic production. Anthropogenic ^{14}C production increased to $0.36 \cdot 10^{26}$ atoms in 2000 then remained largely constant until 2007. Our calculation includes ^{14}C released from nuclear power plants as methane since these releases will eventually oxidize to form $^{14}CO_2$. This assumes that the nuclear-derived atmospheric $^{14}CH_4$ inventory did not change substantially, which is reasonable considering the increase in production was modest over 1992–2000 (30%) and steady thereafter. We assume an uncertainty of ±50% in the total production of ^{14}C by the nuclear energy industry.

[24] Finally, the trend in tropospheric $\Delta^{14}C$ caused by stratosphere-troposphere transport was estimated by a two-box model of the stratosphere with a residence time in the lower box of 1 to 1.5 years and a residence time in the upper box of 5 years, with 28% of the stratospheric mass in the upper box, similar to *Randerson et al.* [2002]. Cosmogenic production of ^{14}C in the stratosphere was simulated to occur either mainly in the lower stratosphere (75%) or to be distributed equally between the stratospheric boxes.

4.2. Modeled Influences on Tropospheric $\Delta^{14}C$ Trend

[25] Fossil fuel CO_2 emissions increased from 6.1 to 8.5 Pg C yr^{-1} between 1992 and 2007, ranging between −0.6 to 5.3% growth each year [*Marland et al.*, 2008; *Canadell et al.*, 2007]. The resulting trend in tropospheric $\Delta^{14}C$ was -11.4 ± 1.1 ‰ yr^{-1} in 1992 and decreased to -13.2 ± 1.3 ‰ yr^{-1} in 2007 (Figure 4a and Table 1). The $\Delta^{14}C$ trend caused by fossil fuel emissions changed by a smaller fraction than the emissions themselves because rising CO_2 concentrations and declining $\Delta^{14}C$ in CO_2 are reducing the sensitivity of atmospheric $\Delta^{14}C$ to fossil fuel-derived CO_2 [*Graven et al.*, 2012; *Levin et al.*, 2010].

[26] Air-sea fluxes contributed to a decreasing trend in $\Delta^{14}C$ and showed the largest change over 1992–2007, from -8.7 ± 2.0 ‰ yr^{-1} in 1992 to -2.4 ± 1.6 ‰ yr^{-1} at the end of 2007 (Figure 4a and Table 1). The disequilibrium between mixed layer and tropospheric $\Delta^{14}C$ as predicted by the box diffusion model shrank from -69 ± 22 ‰ in 1992 to -21 ± 15 ‰ at the end of 2007. In comparison, the simulated disequilibrium of the preindustrial state was -58 ± 7 ‰, which matches observations through our tuning of the model (Section 4.1). The air-sea flux may be considered to consist of a steady state component that roughly balances cosmogenic production and an anthropogenic component that responds to $\Delta^{14}C$ perturbations from nuclear sources of ^{14}C and from ^{14}C dilution by fossil fuel emissions. The air-sea disequilibrium is now weaker than the preindustrial air-sea disequilibrium in our box model simulations, suggesting that the total oceanic uptake of ^{14}C may have become smaller than cosmogenic production in recent years. This indicates that the anthropogenic ^{14}C flux reversed sign. While net removal of ^{14}C from the atmosphere continued through 2007, dilution by fossil fuel CO_2 may have become a stronger influence on the anthropogenic air-sea ^{14}C flux than bomb-derived excess ^{14}C.

[27] The biospheric contribution to the trend in tropospheric $\Delta^{14}C$ was simulated to be relatively constant, 3.7 ± 1.3 ‰ yr^{-1} in 1992 and 4.6 ± 1.2 ‰ yr^{-1} at the end of 2007 (Figure 4a and Table 1). In contrast to the ocean, the disequilibrium between the terrestrial biosphere and the troposphere remained relatively constant from 1992 through 2007 at $+85 \pm 26$ to $+99 \pm 8$ ‰. This is because mean $\Delta^{14}C$ in respired carbon has stopped rising and is now decreasing at

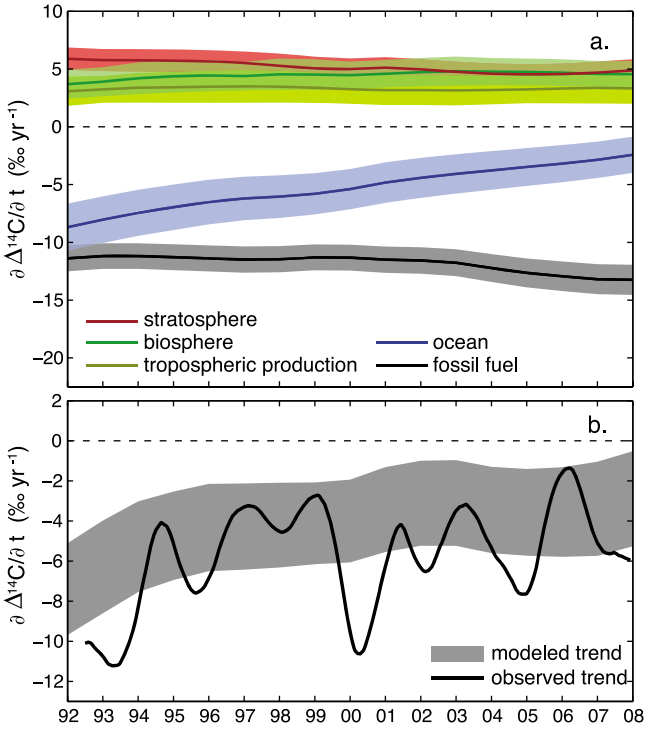

Figure 4. (a) Contributions to the global $\Delta^{14}C$ trend by stratospheric exchange (red), biospheric exchange (green), ^{14}C production in the troposphere (yellow), oceanic exchange (blue) and fossil fuel combustion (black). The filled areas reflect the uncertainty or range of plausible values included in the models for each process and the lines show the middle of the range. (b) The sum of the modeled components is shown as the gray filled area, where the area encompasses the sum of the trends in Figure 4a plus and minus a quadrature sum of the range/uncertainty for each independent process. The derivative of the seasonally adjusted observations at La Jolla is shown by the black line in Figure 4b, repeated from Figure 2b.

a similar rate as tropospheric CO_2 (Section 5.1 and *Naegler and Levin* [2009]).

[28] In order to match the bomb-^{14}C inventory of $615 \pm 35 \cdot 10^{26}$ atoms, simulations of the biosphere model with relatively high NPP were balanced by high biomass, or vice versa, so that fixing one parameter reduced the range of acceptable values for the other parameters. Therefore, if the uncertainty in one of these parameters was improved, the uncertainty in the other parameters could be tightened using the ^{14}C inventory as a constraint.

[29] Using the global inventory of bomb-derived ^{14}C as a constraint also coupled the biospheric parameters to the modeled oceanic inventory. Simulations with slower gas exchange and diffusion reduced the oceanic inventory, requiring longer biospheric residence times to increase the biospheric inventory. Thus, reduced uncertainty in the oceanic bomb ^{14}C inventory or better constraints on the rates of global average air-sea gas exchange and on vertical mixing in the oceanic interior would also tighten the range of acceptable values in the biospheric parameters.

[30] Tropospheric production of ^{14}C by cosmogenic and anthropogenic sources contributed an average of 3.3 ± 1.3 ‰ yr^{-1} to the trend of $\Delta^{14}C$ in the global troposphere (Figure 4a). Cosmogenic production in the troposphere, modeled as 33–50% of total cosmogenic production, comprised an average of 2.5 ± 0.8 ‰ yr^{-1}. Solar variability associated with the sunspot cycle enhanced production in 1993–99 and 2006–08 and reduced production in 1992 and 2000–05 but resulted in only ± 0.2 ‰ yr^{-1} variation in the $\Delta^{14}C$ trend. Production of ^{14}C by nuclear power plants and nuclear fuel reprocessing contributed an average of 0.9 ± 0.5 ‰ yr^{-1}. Decay of ^{14}C in the troposphere is also included in the tropospheric production component of Figure 4a, though decay was only -0.1 ‰ yr^{-1} over the 1992–2007 period.

[31] According to the 2-box model of the stratosphere, the transport of ^{14}C-enriched stratospheric air was a positive influence of 5.9 ± 1.0 ‰ yr^{-1} in 1992 that decreased to 4.9 ± 1.0 ‰ yr^{-1} at the end of 2007 (Figure 4a and Table 1). The decrease in stratospheric influence was consistent with a slowing in the rate of decrease of tropospheric $\Delta^{14}C$ between 1992 and 1997. After this time $\Delta^{14}C$ in the troposphere decreased at a relatively steady rate and the stratospheric contribution to the trend remained relatively constant. After 1997, approximately 30% of the positive influence from the stratosphere was due to the lag time for mixing of tropospheric and stratospheric air and 70% was due to cosmogenic production. In the future, the cosmogenic influence on $\Delta^{14}C$ in the stratosphere and the troposphere is

Table 1. Simulated Contributions to the Tropospheric $\Delta^{14}C$ Trend (‰ yr^{-1}) From This Work and From *Levin et al.* [2010] in 1992 and the End of 2007[a]

	This Work			*Levin et al.* [2010]		
Component	1992	2007	Description	1992	2007	Description
Fossil fuel	−11.4	−13.2	*Marland et al.* [2008]	−11.7	−13.5	*Marland et al.* [2007]
Ocean	−8.7	−2.4	Box diffusion model	−8.7	−1.8	Extrapolation of ocean data
Biosphere	+3.7	+4.6	1-box model	+4.0	+3.5	2-box model
Stratosphere (Transport and Cosmogenic Prod.)	+5.9	+4.9	2-box model and scaled neutron flux data	+6.0	+4.8	16-box model and sinusoidal approx.
Troposphere (Nuclear and Cosmogenic Prod.)	+3.1	+3.3	Scaled nuclear power prod. and scaled neutron flux data	+2.8	+3.5	Extrapolation of *UNSCEAR* [2000] and sinusoidal approx.
Total	−7.4	−2.9		−7.5	−3.5	

[a]Uncertainties are omitted here for clarity but described in Sections 4.2 and 5.1 and shown in Figure 4 for this work.

expected to decline as greater CO_2 concentrations will cause stronger dilution of cosmogenic ^{14}C.

[32] The sum of all contributions to the global $\Delta^{14}C$ trend is shown by the filled area in Figure 4b. The range of values was calculated by adding together the middle of the range of each contribution (shown as lines in Figure 4a) and computing a quadrature sum using one-half of the range of values for each independent process. Simulated ranges in the trend from fossil fuel combustion, ^{14}C production from the nuclear energy industry and the turnover rate of the stratospheric box model each made independent contributions to uncertainty. The range of values for the sum of the biospheric and oceanic components of the trend made a single contribution to the uncertainty in the overall trend, since the biospheric and oceanic parameters of the box models were determined in concert. Similarly, as different estimates shifted cosmogenic ^{14}C production between the stratosphere and troposphere, the range in the sum of cosmogenic production in the stratosphere and troposphere was also considered to be a single contribution to uncertainty.

[33] The global $\Delta^{14}C$ trend predicted by the sum of components weakened slightly between 1992 and 1996 then remained fairly steady between 1997 and 2007. The predicted global trend was -7.4 ± 2.3 ‰ yr^{-1} in 1992 and -2.9 ± 2.4 ‰ yr^{-1} at the end of 2007, averaging -4.2 ± 2.2 ‰ yr^{-1} over the entire period.

[34] The observed, smoothed trend at La Jolla is also shown in Figure 4b, repeated from Figure 2b. The observed trend overlaps the modeled trend except when $\Delta^{14}C$ decreased more rapidly than average, particularly in 1992–93, 2000, and 2004–05. The average trend in $\Delta^{14}C$ observed at La Jolla, -5.5 ± 0.1 ‰ yr^{-1}, lies within the modeled range of values though it is near to the lower end. Consistent with the model, observed trends in $\Delta^{14}C$ show a slower rate of decrease in the recent decade (Section 3 and *Levin et al.* [2010] and *Graven et al.* [2012]).

5. Discussion

5.1. Tropospheric $\Delta^{14}C$ Trend

[35] The correspondence between the modeled global trend and the observed long-term trend at La Jolla suggests that the simple formulations we have used to represent the exchanges of carbon and ^{14}C provide a reasonable description of recent $\Delta^{14}C$ dynamics. As the observed trend is near the lower end of the modeled range, the majority of our simulations are likely to have overestimated the positive trend contributions of the biosphere, stratosphere and/or production in the troposphere and underestimated the negative trend contributions of the ocean and/or fossil fuels.

[36] Simulated trends may be biased by the simplicity of the models, particularly for the ocean and biosphere. The box diffusion model used here does not simulate intermediate or deep water ventilation in high latitudes by allowing direct exchange between the atmosphere and sub-surface oceanic boxes [*Oeschger et al.*, 1975], unlike some other box model formulations [e.g., *Siegenthaler*, 1983]. While the model parameters were selected to correspond to oceanic bomb ^{14}C and anthropogenic carbon inventories, neglecting 3-D transports could overestimate surface $\Delta^{14}C$ in recent years by excluding high latitude exchange with dense, ^{14}C-depleted water. Additionally, the biospheric enrichment predicted by our one-box model is larger than that estimated by *Naegler and Levin* [2009] using a two-box model. This suggests the release of ^{14}C by terrestrial ecosystems may be overestimated, although the discrepancy with *Naegler and Levin* [2009] is reduced by the fact that our one-box model neglects the fraction of NPP (roughly 1/3) which involves rapid turnover of assimilated carbon.

[37] A similar study of the recent trends in $\Delta^{14}C$ was conducted by *Levin et al.* [2010] using a different box model setup, summarized in Table 1. In comparison to *Levin et al.* [2010], our treatment is slightly more complex for air-sea exchange and ^{14}C production and simpler for stratospheric and biospheric exchanges. *Levin et al.* [2010] extrapolated surface $\Delta^{14}C$ from oceanic survey data to estimate air-sea ^{14}C fluxes. Their estimated fluxes were similar to the box diffusion model in 1992 but changed more rapidly over 1992–2007 so that their oceanic contribution to the $\Delta^{14}C$ trend was weaker than our box diffusion model in 2007, though both estimates lie within the other estimate's uncertainty. *Levin et al.* [2010] also extrapolated ^{14}C production by the nuclear energy industry after 1997 and assumed a sinusoidal solar cycle variation in cosmogenic production. As nuclear production increased by only 7% from 1997 to 2007, *Levin et al.*'s [2010] extrapolation is likely to have overestimated production from nuclear power plants in recent years. *Levin et al.*'s [2010] smooth sinusoidal approximation likely underestimated the sharp fluctuations in cosmogenic production, so that production was too strong during solar maxima when cosmogenic production is reduced, particularly the strong solar maximum in 1991–92, and too weak during solar minima when cosmogenic production is enhanced, though the discrepancy is smaller than the total uncertainty. The biospheric ^{14}C flux in *Levin et al.* [2010] was the same as *Naegler and Levin*'s [2009] two-box model, as previously mentioned, and simulated a positive contribution that was within 1 ‰ yr^{-1} of our one-box model. The biospheric contribution decreased slightly in *Naegler and Levin*'s [2009] model over 1992–2007 while the biospheric contribution increased slightly, on average, in our one-box model (Table 1). The different tendencies reflect a small growth in the troposphere-biosphere disequilibrium in our one-box model versus a small reduction in the troposphere-biosphere disequilibrium in the two-box model between 1992 and 2007, suggesting the discrepancy between the one-box and two-box models is likely to be larger outside of the 1992–2007 interval considered here. Positive contributions of 5–6 ‰ yr^{-1} were simulated over 1992–2007 by both the 2-box stratosphere model we used and *Levin et al.*'s [2010] 16-box stratosphere. Both models used fossil fuel emission data from *Marland et al.* [2008] leading to similar contributions to the $\Delta^{14}C$ trend. Differences in the fossil fuel component are likely due to small differences in the estimated global mean atmospheric composition or the size of the troposphere.

[38] The simulated components of the $\Delta^{14}C$ trend and the total $\Delta^{14}C$ trend in this work and in the work by *Levin et al.* [2010] are nearly the same (Table 1), despite the differences in model formulation. The average global trend

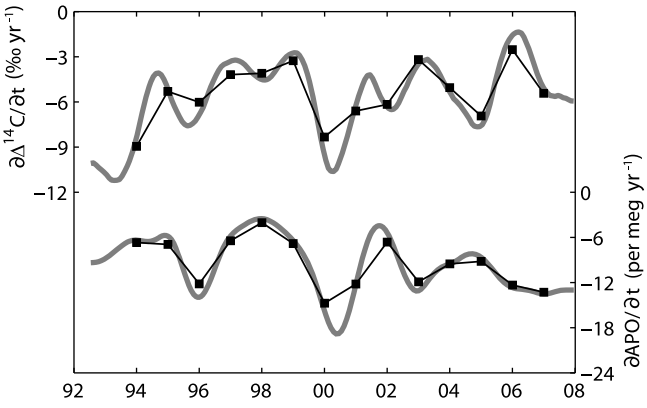

Figure 5. The derivative of the seasonally adjusted observations at La Jolla for (top) $\Delta^{14}C$ (repeated from Figure 2b) and (bottom) APO [*Hamme and Keeling*, 2008], shown as gray lines. The change in annual mean $\Delta^{14}C$ and APO at La Jolla is shown by the black squares.

simulated over 1992–2007 was −4 ‰ yr^{-1} in our model and −5 ‰ yr^{-1} in that of *Levin et al.* [2010], consistent within the uncertainty of ±2–3 ‰ yr^{-1}. We note however that both model setups have used *Naegler and Levin*'s [2006] estimate of total bomb-derived excess ^{14}C as a constraint on biospheric and oceanic $\Delta^{14}C$, and that the simulated trends have rather large uncertainties (Section 4.2 and *Levin et al.* [2010]). The average global trend over 1992–2007 is smaller in our model, despite matching that of *Levin et al.* [2010] in 1992 (Table 1), since *Levin et al.*'s [2010] simulated trend weakens gradually over the whole period while our simulated trend weakens more rapidly in the first few years then remains fairly steady. The largest component of uncertainty to the trend is in air-sea exchange, suggesting that additional constraints on the air-sea flux of ^{14}C would particularly improve the uncertainty range of the full modeled trend of $\Delta^{14}C$.

5.2. Rapid Decline of $\Delta^{14}C$ in 2000

[39] The most outstanding feature in the seasonally adjusted $\Delta^{14}C$ record at La Jolla is the rapid decrease in $\Delta^{14}C$ in 2000 (Figures 2b and 4b). The rate of decrease appeared to be nearly twice as rapid as the average. The feature was also observed at Jungfraujoch, Switzerland but not at Cape Grim, Australia [*Levin et al.*, 2010], suggesting it extended through the Northern Hemisphere midlatitudes but not into the Southern Hemisphere. Restriction to the Northern Hemisphere suggests that anomalous regional ^{14}C or carbon fluxes or changes in atmospheric circulation in northern regions may be responsible for the enhanced decline in $\Delta^{14}C$.

[40] One potential cause of the anomalous decrease in Northern midlatitude $\Delta^{14}C$ in 2000 may have been a strengthening of the regional air-sea ^{14}C flux in the Northern Pacific Ocean. In 2000–01, winter sea surface temperature in the Pacific north of 40° was anomalously cold and high wind speeds and exceptionally high gas exchange velocities were observed in the Western North Pacific [*Kawabata et al.*, 2003]. These high wind speeds may have enhanced the ventilation of deep waters in the North Pacific, exposing aged and ^{14}C-poor water masses [*Key et al.*, 2004] and resulting in rapid, anomalous net exchange with lower-$\Delta^{14}C$ CO_2 entering the atmosphere and higher-$\Delta^{14}C$ CO_2 entering the ocean. Direct observations are not available to verify that changes in $\Delta^{14}C$ occurred in the surface waters of the North Pacific during this time period. However, this process can be investigated with observations of atmospheric O_2, since anomalous ventilation would also enhance oceanic uptake of O_2, which is depleted in aged water masses due to consumption by organic matter remineralization.

[41] *Hamme and Keeling* [2008] observed a strong decrease in atmospheric oxygen in the Northern Hemisphere during 1999–2001 that is concurrent with the strong decrease in our $\Delta^{14}C$ observations at La Jolla. In Figure 5, we show the trend over 1992–2007 in seasonally adjusted $\Delta^{14}C$ and atmospheric O_2/N_2 ratios, given as atmospheric potential oxygen (APO). The APO notation refers to O_2/N_2 ratios that have been corrected for terrestrial biospheric exchange, reported as part per million deviations from a standard ratio [*Stephens et al.*, 1998; *Keeling et al.*, 1998]. We also show the year-to-year change in annual mean to demonstrate that the anomalous decline of both $\Delta^{14}C$ and APO in 2000 is not likely to be an artifact of curve fitting procedures. The year-to-year change in annual mean also shows an anomalous decrease in both $\Delta^{14}C$ and APO, though the anomalies are reduced due to the coarser temporal resolution in the annual mean compared to the spline curves.

[42] *Hamme and Keeling* [2008] estimate that anomalous exposure of deep waters with potential density of 1026.6 kg m^{-3} (the σ_θ 26.6 isopycnal) in the Western North Pacific could account for the decrease observed in atmospheric O_2/N_2. Using the approximations of *Hamme and Keeling* [2008] to account for the air-sea O_2 flux, we estimate that the decrease in $\Delta^{14}C$ could also be explained by unusual exposure of and rapid exchange with cool, deep waters in the North Pacific. $\Delta^{14}C$ in waters of the σ_θ 26.6 isopycnal was observed to be −20 ‰ in 1992 [*Key et al.*, 2004], approximately 30 ‰ lower than $\Delta^{14}C$ in waters of the σ_θ 26.4 and 26.5 isopycnals that normally outcrop in the Western North Pacific near the Kamchatka Peninsula. Assuming that $\Delta^{14}C$ in these isopycnals did not change substantially between 1992 and 2000, the exposure of the σ_θ 26.6 isopycnal would have enhanced the local air-sea $\Delta^{14}C$ gradient by 30–40%. The resulting increase in ^{14}C flux could potentially have caused an anomalous decrease of −1 to −4.5 ‰ yr^{-1} in Northern midlatitude air, depending on the spatial extent of anomalous upwelling and the advection and mixing of the low-$\Delta^{14}C$ air from the Pacific. A model study resolving high frequency changes to air-sea fluxes and atmospheric transport from the ocean surface is needed to accurately test this hypothesis.

[43] Anomalies in oceanic fluxes occurring in the tropics are not likely to be responsible for the anomalous decrease in $\Delta^{14}C$ in 2000 or other significant variability in the recent trend of $\Delta^{14}C$ at La Jolla because the tropical air-sea $\Delta^{14}C$ gradient observed in the 1990s was weak. Surface waters of the equatorial Eastern Pacific during the 1990s had $\Delta^{14}C$ of approximately 70 ‰, as measured in dissolved inorganic

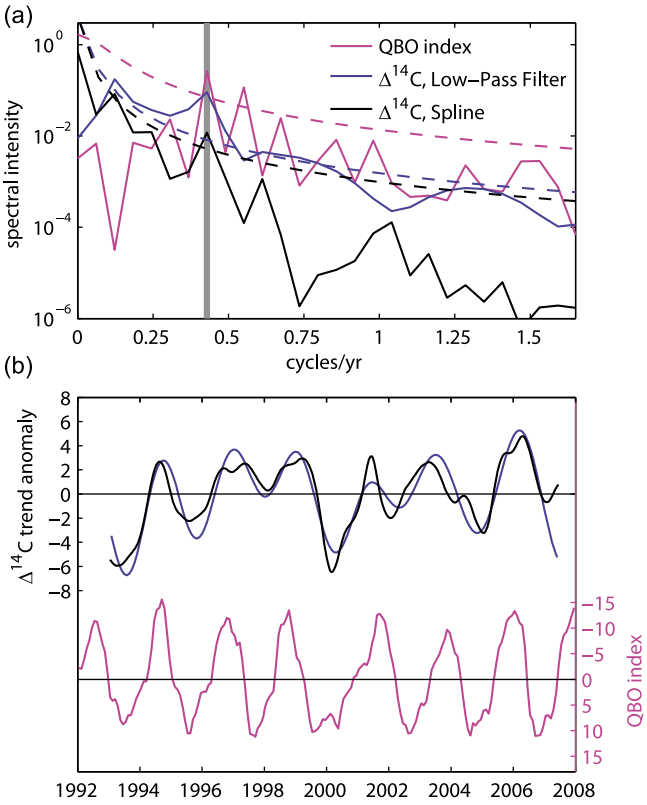

Figure 6. (a) Power spectra of the QBO index and of linearly detrended, seasonally adjusted $\Delta^{14}C$ at La Jolla using low-pass filter and spline techniques as solid lines. Dashed lines show corresponding red noise spectra. The 28-month period is indicated by the vertical gray line. (b) The $\Delta^{14}C$ trend anomaly and QBO index for 1992–2007, where the axis of the QBO index is inverted. The QBO index shows the zonally averaged 50 hPa zonal wind anomaly at the equator in m s^{-1} (available at http://www.cpc.ncep.noaa.gov/data/indices/).

carbon by *Nydal et al.* [1998] and *Key et al.* [2004] and in shallow corals at Wolf Island by T. Guilderson. This was only 30 ‰ lower than average atmospheric $\Delta^{14}C$ in 2000. By contrast, $\Delta^{14}C$ in the σ_θ 26.6 isopycnal water of the North Pacific was roughly 125 ‰ below atmospheric $\Delta^{14}C$. Moreover, the anomalous drop in atmospheric $\Delta^{14}C$ in 2000 was not observed at Cape Grim, Australia [*Levin et al.*, 2010], suggesting the cause of the anomaly took place in northern regions.

[44] The rate of decrease in $\Delta^{14}C$ observed at La Jolla in 1992–93 also appeared to be quite rapid, with $\Delta^{14}C$ dropping at a similar rate as in 2000. The anomaly in 1993 was probably smaller in magnitude than in 2000, however, since an overall slowing in the rate of decrease of $\Delta^{14}C$ occurred between 1993 and 2000. Observations at Jungfraujoch show a similar rate of decrease in 1992–93 as at La Jolla (−10 ‰ yr^{-1}), but the trend of $\Delta^{14}C$ in the longer record at Jungfraujoch clearly slowed between 1986 and 2000 such that the trend observed in 1992–93 was not especially prominent [*Levin et al.*, 2010].

5.3. Periodic Variation in $\Delta^{14}C$

[45] To identify timescales of periodic variability we performed a spectral analysis on $\Delta^{14}C$ at La Jolla after adjusting the observations to regularly spaced monthly values and linearly detrending. The monthly values were calculated by fitting a function to the observations that included a linear trend, an annual harmonic and an error term that was evaluated using a loose spline (cutoff period of 4 months), and then evaluating the function at mid-month. A power spectrum of the $\Delta^{14}C$ observations expressed a strong peak at an annual period; we investigate this seasonal variation in an accompanying paper [*Graven et al.*, 2012]. A smaller peak was also present at a period of 28 months.

[46] Variation in $\Delta^{14}C$ of atmospheric CO_2 at the 28 month (2.3 yr) period has not previously been reported. Variation on periods of 2.6–5.8 yr at Wellington, New Zealand over 1970–1995 was described by *Dutta* [2002], and related to perturbations in air-sea exchanges [*Rozanski et al.*, 1995] and, potentially, air-land exchanges caused by the El Niño/Southern Oscillation.

[47] The smaller peak at the 28-month period can be investigated by comparing a spectrum of the $\Delta^{14}C$ data, after removing the seasonal variation, with the corresponding red noise spectrum with the same one-lag autocorrelation coefficient [*Wilks*, 1995]. The seasonal variation was removed from the data in two ways. First, by using the spline curve described in Section 3. Second, by applying a low-pass Butterworth filter with 10th order and cutoff period of 24 months. In both methods, the 28-month period was outside the 0.05 confidence interval of the corresponding red noise spectra (Figure 6a), suggesting that observed variability at this period is real and significant. Variation at 2–3 year timescales is also apparent in the observed trend (Figures 2b and 6b) and suggests that $\Delta^{14}C$ may be sensitive to climatic variations that operate on similar timescales.

[48] One climatic mode that may be associated with $\Delta^{14}C$ variability of a 28 month period is the Quasi-Biennial Oscillation (QBO), a periodic shifting of the zonal winds in the tropical stratosphere that regulate tropical upwelling into the stratosphere and the planetary waves that influence extratropical tropospheric weather patterns and stratosphere-troposphere exchange [*Baldwin et al.*, 2001]. The QBO's dominant period is also 28 months, the same period observed in $\Delta^{14}C$ at La Jolla (Figure 6a). In an atmospheric transport modeling study, *Hamilton and Fan* [2000] found that the QBO had a significant influence on simulated tropospheric growth rates of long-lived trace gases N_2O and CH_4 through its influence on stratosphere-troposphere transport, suggesting the QBO may also have significant effects on $\Delta^{14}C$ variability. The effects of the QBO on $\Delta^{14}C$ variability are likely to be opposite to the effects on N_2O and CH_4, since the stratosphere is a source for ^{14}C and a sink for N_2O and CH_4. Figure 6b shows that positive anomalies in the trend of $\Delta^{14}C$ at La Jolla appear to coincide with negative anomalies in the QBO index at 50 hPa, which correspond to easterly winds and enhanced upwelling in the tropical stratosphere. The mechanism by which the QBO could modulate the tropospheric growth rate of $\Delta^{14}C$ may be associated with the transport of tropospheric, low-$\Delta^{14}C$ air into the stratosphere in the tropics, or with the transport of stratospheric, high-$\Delta^{14}C$ air into the troposphere in the

extratropics, and may involve substantial lags [*Hamilton and Fan*, 2000]. Studies using an atmospheric model would allow potential mechanisms of interaction between the QBO and tropospheric $\Delta^{14}C$ to be investigated.

6. Summary

[49] Measurements of $\Delta^{14}C$ in CO_2 were conducted on monthly samples from La Jolla, California, USA collected between July 1992 and December 2007 by the Scripps CO_2 Program. $\Delta^{14}C$ analysis was conducted at Lawrence Livermore National Laboratory by accelerator mass spectrometry with average measurement uncertainty of ±1.9 ‰.

[50] The $\Delta^{14}C$ observations fit an average linear trend of -5.5 ± 0.1 ‰ yr^{-1}. The decrease of $\Delta^{14}C$ was highly variable, however, and expressed a 28-month periodicity. A strong decline in $\Delta^{14}C$ in 2000 was concurrent with a strong decline in atmospheric O_2/N_2 ratios at La Jolla, suggesting a mutual cause from enhanced oceanic ventilation in the North Pacific [*Hamme and Keeling*, 2008].

[51] Using simple models of the contributions to the global tropospheric $\Delta^{14}C$ trend, similar to *Levin et al.* [2010], we showed that fossil fuel emissions were the strongest influence between 1992 and 2007. Oceanic exchange also contributed a negative influence over the entire period 1992–2007; however, the influence weakened by 70%. The modeled air-sea ^{14}C flux and $\Delta^{14}C$ disequilibrium is now smaller than in the preindustrial state, suggesting the perturbation caused by fossil fuel emissions appears to have become more important than the perturbation from nuclear weapons testing. Negative influences from fossil fuel combustion and oceanic exchange were moderated by ^{14}C production in the troposphere and biospheric and stratospheric exchange, adding up to an overall rate of change of -4.1 ± 2.2 ‰ yr^{-1}, slower than the average observed trend but consistent within the uncertainties.

Appendix A: Data Table

[52] Measurements of $\Delta^{14}C$ in CO_2 samples collected by the Scripps CO_2 Program and measured at Lawrence Livermore National Laboratory are provided in Table A1. The CO_2 mole ratio and $\delta^{13}C$ listed are an average of all measurements with the same sample date. The $\delta^{13}C$ values footnoted with an "a" in Table A1 are estimates of $\delta^{13}C$ when measurements of $\delta^{13}C$ in concurrently sampled CO_2 were not available. CO_2 mole ratios were measured on the 'SIO 2008A' Calibration Scale. The SIO calibration scale for CO_2 is established by infrared and manometric analysis of primary reference gases [*Keeling et al.*, 2002]. The SIO calibration scale is tied to the historic CO_2 measurements at SIO and independent of the WMO scale since 1995. $\delta^{13}C$ values are relative to the international V-PDB standard and include the addition of a −0.112 ‰ offset for consistency with measurements performed at the Center for Isotope Research, University of Groningen, Netherlands. σ_{Tot} is the total measurement uncertainty in $\Delta^{14}C$. Flagged samples (14%) have been removed. $\Delta^{14}C$ measurements at 6 additional SIO clean air sites are reported in the companion paper [*Graven et al.*, 2012].

Table A1. Measurements From La Jolla, California, USA

SIO ID	LLNL ID	Sample Date	CO_2 (ppm)	$\delta^{13}C$ (‰)	$\Delta^{14}C$ (‰)	σ_{Tot} (‰)
K92-418	116193	01-Jul-92	355.35	−7.815	135.0	1.7
K92-487	124125	23-Jul-92	351.31	−7.605	131.5	1.7
K92-496	116194	03-Aug-92	352.50	−7.671	133.7	1.7
K92-840	116195	09-Sep-92	348.56	−7.514	137.6	1.7
K93-004	116196	02-Oct-92	351.67	−7.667	135.2	1.7
K93-023	116197	29-Oct-92	354.58	−7.780	132.5	1.7
K93-059	116199	11-Dec-92	358.68	−8.046	128.7	1.7
K93-081	124395	18-Dec-92	358.76	−8.003	132.3	1.7
K93-141	116200	11-Jan-93	359.76	−8.058	129.4	1.7
K93-149	116201	09-Feb-93	359.41	−8.039	132.8	1.7
K93-208	124402	24-Feb-93	360.03	−8.065	127.7	1.7
K93-237	116202	03-Mar-93	360.59	−8.087	129.9	1.7
K93-245	116204	12-Apr-93	360.79	−8.027	125.2	1.7
K93-356	116205	18-May-93	362.35	−8.106	127.8	1.7
K93-431	116206	21-Jun-93	359.62	−7.952	127.3	1.7
K93-502	124121	01-Jul-93	357.25	−7.862	120.5	1.7
K93-612a	128108	12-Aug-93	351.71	−7.569	123.4	1.7
K93-612b	128112	12-Aug-93	351.71	−7.569	124.8	1.7
K93-979	131551	11-Nov-93	356.26	−7.810	125.0	1.7
K94-107	124385	30-Nov-93	357.98	−7.917	121.4	1.7
K94-253a	131029	15-Dec-93	359.93	−8.018	119.6	1.7
K94-298	124366	08-Feb-94	360.76	−8.034	116.1	1.7
K94-355	131095	11-Mar-94	360.94	−8.024	119.7	1.7
K94-402	124122	04-Apr-94	362.71	−8.174	111.8	1.7
K94-675	124123	17-May-94	363.79	−8.222	115.2	1.7
K94-729	124126	22-Jun-94	359.73	−7.987	115.1	1.7
K94-952	124128	24-Aug-94	352.63	−7.627	114.9	1.7
K94-951	116209	24-Aug-94	352.63	−7.627	118.5	1.7
K95-006	124136	02-Nov-94	358.39	−7.890	118.7	1.7
K95-018	116212	18-Nov-94	360.65	−8.014	118.7	1.7
K95-179	116215	03-Jan-95	361.47	−8.066	119.4	1.7
K95-581	116216	08-Feb-95	362.79	−8.150	116.8	1.7
K95-587	124137	15-Feb-95	362.54	−8.186	110.3	1.7
K95-724	116217	13-Mar-95	363.59	−8.181	113.4	1.7
K95-755	116218	07-Apr-95	363.60	−8.141	109.0	1.7
K95-846	116219	15-May-95	365.56	−8.247	114.5	1.7
K95-851	101933	08-Jun-95	363.99	−8.275	109.5	2.3
K95-850	104335	08-Jun-95	363.99	−8.275	112.4	2.3
K95-852	116220	08-Jun-95	363.99	−8.275	113.8	1.7
K95-A48	104336	03-Jul-95	360.79	−7.966	112.4	2.4
K95-A49	101934	03-Jul-95	360.79	−7.966	112.9	2.2
K95-C89	124160	21-Aug-95	353.10	−7.578	107.9	1.7
K95-C87	101935	21-Aug-95	353.10	−7.578	110.2	2.2
K95-C86	104337	21-Aug-95	353.10	−7.578	110.2	2.3
K95-E07	104338	26-Sep-95	357.76	−7.809	106.5	2.4
K95-E08	101936	26-Sep-95	357.76	−7.809	108.3	2.2
K96-023	101937	16-Oct-95	358.38	−7.790	107.9	2.3
K96-022	104339	16-Oct-95	358.38	−7.790	112.5	2.3
K96-035	101938	10-Nov-95	360.49	−7.939	108.5	2.2
K96-034	104340	10-Nov-95	360.49	−7.939	109.7	2.3
K96-132	103195	22-Jan-96	364.56	−8.153	105.0	2.2
K96-131	103194	22-Jan-96	364.56	−8.153	106.8	2.2
K96-149a	124406	02-Feb-96	365.31	−8.154	112.8	1.7
K96-149b	124407	02-Feb-96	365.31	−8.154	116.1	1.7
K96-185	103196	22-Feb-96	365.91	−8.224	103.9	2.3
K96-187	124124	22-Feb-96	365.91	−8.224	104.1	1.7
K96-186	103197	22-Feb-96	365.91	−8.224	104.2	2.2
K96-297	103199	11-Mar-96	365.16	−8.171	104.6	2.1
K96-296	103198	11-Mar-96	365.16	−8.171	107.8	2.2
K96-321	124158	01-Apr-96	366.10	−8.217	103.0	1.7
K96-378	103201	16-Apr-96	366.48	−8.222	102.5	2.2
K96-377	103200	16-Apr-96	366.48	−8.222	105.2	2.2
K96-450	103202	03-May-96	367.60	−8.204	102.2	2.2
K96-451	103203	03-May-96	367.60	−8.204	106.1	2.2
K96-518	103204	26-Jun-96	363.05	−8.027	104.1	2.2
K96-519	104346	26-Jun-96	363.05	−8.027	104.3	2.3
K96-711	124162	05-Aug-96	358.46	−7.775	104.0	1.7
K96-837	124381	04-Sep-96	356.25	−7.680	105.4	1.7
K96-921	131538	25-Oct-96	361.37	−7.942	108.1	1.7
K96-938	124171	27-Nov-96	364.09	−8.075	104.8	1.7
K97-112	141146	03-Jan-97	364.45	−8.137	101.5	2.2

Table A1. (continued)

SIO ID	LLNL ID	Sample Date	CO_2 (ppm)	$\delta^{13}C$ (‰)	$\Delta^{14}C$ (‰)	σ_{Tot} (‰)
K97-150	124172	17-Feb-97	365.88	−8.161	98.9	1.7
K97-151	124380	17-Feb-97	365.88	−8.161	101.4	1.7
K97-213	131110	22-Apr-97	367.81	−8.170	100.2	1.7
K97-375	124174	23-Jun-97	364.68	−8.053	100.7	1.7
K97-381	124400	30-Jun-97	363.74	−8.022	103.4	1.7
K97-465	124178	18-Jul-97	359.32	−7.752	99.2	1.7
K97-466	138143	18-Jul-97	359.32	−7.752	103.9	2.2
K97-569	131570	10-Aug-97	357.23	−7.634	102.5	1.7
K97-660b	128095	10-Oct-97	360.19	−7.792	101.3	1.7
K97-660a	128074	10-Oct-97	360.19	−7.792	101.7	1.7
A98-005	124177	10-Jan-98	365.99	−8.092	101.3	1.7
A98-011	124367	13-Jan-98	367.52	−8.180	100.3	1.7
K98-102b	126937	13-Feb-98	367.29	−8.150	97.4	1.7
K98-102a	126910	13-Feb-98	367.29	−8.150	99.0	1.7
A98-183	125613	23-Apr-98	370.04	−8.297	96.6	1.7
A98-197	124212	22-May-98	370.58	−8.312	92.5	1.7
A98-198	124388	22-May-98	370.58	−8.312	93.3	1.7
A98-272	101940	29-Jun-98	364.02	−7.958	96.6	2.2
A98-474	125579	29-Jul-98	363.43	−7.884	95.1	1.7
A98-473	101942	29-Jul-98	363.43	−7.884	98.9	2.2
A98-472	101941	29-Jul-98	363.43	−7.884	99.3	2.2
A98-480	101943	25-Aug-98	360.37	−7.759	96.8	2.6
A98-481	101944	25-Aug-98	360.37	−7.759	98.7	2.3
A99-040	101945	29-Oct-98	366.91	−8.094	97.1	2.2
K99-029	101946	29-Oct-98	366.91	−8.094	97.9	2.2
K99-035	101948	14-Dec-98	370.09	−8.264	95.1	2.5
A99-046	101947	14-Dec-98	370.09	−8.264	97.9	2.2
K99-044	101949	26-Jan-99	370.21	−8.268	90.5	2.3
A99-130	101950	26-Jan-99	370.21	−8.268	92.3	2.2
K99-050	138125	08-Feb-99	371.34	−8.288	95.1	2.2
A99-243	124180	12-Apr-99	372.90	−8.353	93.6	1.7
A99-511	125603	21-Jul-99	363.01	−7.842	91.8	1.7
A99-512	124208	21-Jul-99	363.01	−7.842	93.8	1.7
A99-551	125614	10-Aug-99	364.68	−7.881	90.9	1.7
A99-552	125624	10-Aug-99	364.68	−7.881	93.3	1.7
A99-760	124404	08-Sep-99	361.55	−7.751	94.9	1.7
A99-766	126967	15-Oct-99	366.34	−7.979	94.6	1.7
A00-009	124176	16-Nov-99	367.85	−8.044	95.1	1.7
A00-014	124371	17-Nov-99	369.03	−8.125	97.0	1.7
A00-122	125588	31-Dec-99	369.80	−8.130	92.8	1.7
A00-128	127000	21-Jan-00	370.28	−8.129	94.2	1.7
A00-185	125590	11-Feb-00	372.05	−8.267	91.6	1.7
A00-210	141141	22-Feb-00	372.56	−8.285	85.0	2.2
A00-289	138077	20-Mar-00	374.38	−8.348	83.3	2.2
A00-288	124386	20-Mar-00	374.38	−8.348	86.0	1.7
A00-304	124205	14-Apr-00	373.79	−8.335	85.1	1.7
A00-412	124209	26-May-00	374.37	−8.348	83.5	1.7
A00-419	124210	05-Jun-00	372.08	−8.225	83.7	1.7
A00-448	104352	16-Jun-00	371.90	−8.208	81.2	2.2
A00-447	103210	16-Jun-00	371.90	−8.208	81.8	2.2
A00-567	103211	14-Jul-00	365.91	−7.886	85.0	2.2
A00-571	124213	14-Jul-00	365.91	−7.886	85.4	1.7
A00-568	104353	14-Jul-00	365.91	−7.886	85.8	2.3
A00-607	104354	14-Aug-00	362.61	−7.733	82.6	2.2
A00-606	103212	14-Aug-00	362.61	−7.733	83.3	2.2
A00-609	124214	14-Aug-00	362.61	−7.733	83.5	1.7
A00-615	124175	18-Aug-00	360.34	−7.603	87.4	1.7
A00-718	104355	05-Sep-00	362.31	−7.733	82.9	2.2
A00-719	103213	05-Sep-00	362.31	−7.733	85.8	2.2
A00-730	104356	10-Oct-00	367.34	−7.960	84.9	2.2
A00-731	103214	10-Oct-00	367.34	−7.960	85.5	2.2
A01-085	103215	09-Nov-00	370.23	−8.106	83.1	2.3
A01-086	104357	09-Nov-00	370.23	−8.106	84.3	2.1
A01-121	104366	08-Jan-01	372.10	−8.156	83.5	2.2
A01-122	104367	08-Jan-01	372.10	−8.156	84.9	2.3
A01-128	104369	07-Feb-01	373.84	−8.244	79.5	2.1
A01-127	104368	07-Feb-01	373.84	−8.244	80.0	2.1
A01-188	104371	07-Mar-01	375.11	−8.328	75.2	2.2
A01-187	104370	07-Mar-01	375.11	−8.328	75.9	2.4
A01-217	124364	23-Mar-01	373.77	−8.256	77.8	1.7
A01-233	104373	02-Apr-01	375.87	−8.363	73.2	2.1

Table A1. (continued)

SIO ID	LLNL ID	Sample Date	CO_2 (ppm)	$\delta^{13}C$ (‰)	$\Delta^{14}C$ (‰)	σ_{Tot} (‰)
A01-232	104372	02-Apr-01	375.87	−8.363	75.4	2.3
A01-308	104374	04-May-01	376.70	−8.422	73.2	2.2
A01-309	104375	04-May-01	376.70	−8.422	74.2	2.2
A01-302	104376	04-Jun-01	375.73	−8.326	76.2	2.1
A01-303	104377	04-Jun-01	375.73	−8.326	76.2	2.3
A01-298	128062	04-Jun-01	375.73	−8.326	78.2	1.7
A01-358	128093	13-Jun-01	373.27	−8.212	76.8	1.7
A01-363	104342	13-Jun-01	373.27	−8.212	79.4	2.4
A01-362	104341	13-Jun-01	373.27	−8.212	80.0	2.3
A01-383	104343	16-Jul-01	366.73	−7.860	82.5	2.2
A01-382	104334	16-Jul-01	366.73	−7.860	84.6	2.3
A01-574	124217	24-Jul-01	364.55	−7.750	86.0	1.7
A01-584	104344	10-Aug-01	365.22	−7.792	80.9	2.2
A01-585	104345	10-Aug-01	365.22	−7.792	84.1	2.3
A01-599	104381	06-Sep-01	363.82	−7.739	83.3	2.2
A01-598	104380	06-Sep-01	363.82	−7.739	83.8	2.2
A01-613	104383	31-Oct-01	370.02	−8.011	75.9	2.2
A01-609	141173	31-Oct-01	370.02	−8.011	77.0	2.2
A01-612	104382	31-Oct-01	370.02	−8.011	78.5	2.2
A02-092	104384	09-Dec-01	372.87	−8.185	73.5	2.2
A02-093	104385	09-Dec-01	372.87	−8.185	75.6	2.2
A02-170	101951	09-Jan-02	374.34	−8.216	74.6	2.2
A02-165	128065	09-Jan-02	374.34	−8.216	76.9	1.7
A02-169	104386	09-Jan-02	374.34	−8.216	80.1	2.5
A02-186	101952	17-Feb-02	375.21	−8.274	74.0	2.2
A02-185	104387	17-Feb-02	375.21	−8.274	75.1	2.8
A02-225	101953	22-Mar-02	376.98	−8.365	70.9	2.2
A02-224	104388	22-Mar-02	376.98	−8.365	73.6	2.5
A02-221	124218	22-Mar-02	376.98	−8.365	77.1	1.7
A02-254	104389	25-Apr-02	376.87	−8.334	71.5	2.6
A02-255	101954	25-Apr-02	376.87	−8.334	77.3	2.2
A02-353	103192	13-May-02	377.25	−8.332	68.1	2.2
A02-352	101931	13-May-02	377.25	−8.332	68.5	2.3
A02-368	124195	10-Jun-02	375.99	−8.265	75.0	1.7
A02-419	101932	21-Jun-02	373.09	−8.123	68.4	2.4
A02-420	103193	21-Jun-02	373.09	−8.123	69.3	2.2
A02-465	117787	12-Jul-02	371.13	−7.998	72.6	1.7
A02-469	124215	24-Jul-02	368.98	−7.892	74.3	1.7
A02-470	125591	24-Jul-02	368.98	−7.892	79.2	1.7
A02-572	117796	06-Aug-02	364.89	−7.713	74.1	1.7
A02-584	117802	09-Sep-02	367.55	−7.858	70.4	1.7
A02-766	125584	11-Oct-02	371.31	−8.021	72.7	1.7
A02-765	117842	11-Oct-02	371.31	−8.021	72.7	2.9
A03-058	117847	09-Nov-02	372.65	−8.063	70.2	2.7
A03-149	117846	17-Dec-02	375.99	−8.284	70.8	2.8
A03-155	128142	29-Dec-02	376.84	−8.303	69.5	1.7
A03-162	126976	07-Feb-03	378.07	−8.377	66.6	1.7
A03-161	117794	07-Feb-03	378.07	−8.377	75.4	1.7
A03-168	141154	14-Feb-03	378.03	−8.339	71.6	2.2
A03-259	128087	04-Mar-03	377.14	−8.279	71.1	1.7
A03-265	141197	18-Mar-03	379.18	−8.415	67.7	2.2
A03-275	125585	10-Apr-03	379.49	−8.405	65.3	1.7
A03-274	117839	10-Apr-03	379.49	−8.405	66.2	2.7
A03-426	125593	24-Apr-03	380.88	−8.508	71.8	1.7
A03-425	124403	24-Apr-03	380.88	−8.508	76.2	1.7
A03-460	128119	04-Jun-03	380.03	−8.409	69.1	1.7
A03-473	131036	24-Jun-03	376.67	−8.252	67.7	1.7
A03-472	138106	24-Jun-03	376.67	−8.252	70.4	2.2
A03-601	117794	29-Aug-03	367.46	−7.787	68.4	1.7
A03-608	125623	09-Sep-03	367.95	−7.772	71.1	1.7
A03-607	125602	09-Sep-03	367.95	−7.772	73.1	1.7
A04-013	126904	31-Oct-03	375.35	−8.156	69.7	1.7
A04-020	128129	16-Nov-03	377.45	−8.285	65.8	1.7
A04-019	126960	16-Nov-03	377.45	−8.285	67.4	1.7
A04-117	126922	26-Dec-03	379.21	−8.347	67.9	1.7
A04-247	124409	31-Jan-04	380.44	−8.406	69.6	1.7
A04-263	126943	26-Feb-04	380.52	−8.408	63.3	1.7
A04-269	124378	24-Mar-04	381.56	−8.426	61.8	1.7
A04-276	125605	26-Mar-04	380.97	−8.403	65.1	1.7
A04-275	125604	26-Mar-04	380.97	−8.403	66.1	1.7
A04-424	125608	20-Apr-04	382.02	−8.476	62.5	1.7

Table A1. (continued)

SIO ID	LLNL ID	Sample Date	CO_2 (ppm)	$\delta^{13}C$ (‰)	$\Delta^{14}C$ (‰)	σ_{Tot} (‰)
A04-447	125617	26-May-04	379.87	−8.353	63.8	1.7
A04-530	116149	09-Jun-04	380.44	−8.369	61.9	1.7
A04-529	116148	09-Jun-04	380.44	−8.369	63.7	1.8
A04-532	124370	09-Jun-04	380.44	−8.369	66.7	1.7
A04-691	117822	27-Jul-04	374.98	−8.039	64.3	2.7
A04-690	117808	27-Jul-04	374.98	−8.039	66.6	1.7
A04-735	117865	28-Jul-04	373.33	−7.994	60.8	1.7
A04-734	117823	28-Jul-04	373.33	−7.994	62.1	3.3
A04-740	126932	26-Aug-04	369.73	−7.782	66.4	1.7
A04-786	126990	14-Sep-04	370.29	−7.819	66.2	1.7
A04-792	125569	10-Oct-04	375.30	−8.066	60.1	1.7
A04-793	125587	10-Oct-04	375.30	−8.066	62.9	1.7
A05-047	128155	21-Dec-04	380.36	−8.272	65.7	1.7
AORG416	113089	26-Jan-05	380.05	−8.237	58.1	1.7
CDRG249	113085	26-Jan-05	380.05	−8.237	59.4	1.7
CDRG248	113084	26-Jan-05	380.05	−8.237	60.2	1.7
CDRG250	113086	26-Jan-05	380.05	−8.237	60.6	1.7
AORG420	113090	26-Jan-05	380.05	−8.237	60.7	1.7
AORG338	113088	26-Jan-05	380.05	−8.237	61.4	1.7
AORG126	113087	26-Jan-05	380.05	−8.237	61.9	1.7
CDRG247	113083	26-Jan-05	380.05	−8.237	63.3	1.7
A05-236	125622	07-Feb-05	382.09	−8.376	60.3	1.7
AORG262	116168	23-Mar-05	383.41	−8.450	58.6	2.1
CDRG222	116171	23-Mar-05	383.41	−8.450	58.9	1.7
CDRG219	116170	23-Mar-05	383.41	−8.450	60.5	2.2
AORG366	116145	07-Apr-05	383.95	−8.510	54.8	1.7
A05-288	116166	07-Apr-05	383.95	−8.510	55.6	2.2
A05-308	125581	19-Apr-05	384.29	−8.506	51.4	1.7
A05-309	125566	19-Apr-05	384.29	−8.506	51.8	1.7
A05-351	125567	03-May-05	384.02	−8.465	50.5	1.7
A05-349	124394	03-May-05	384.02	−8.465	57.2	1.7
A05-472	125610	18-Jun-05	382.18	−8.375	52.4	1.7
A05-470	125568	18-Jun-05	382.18	−8.375	53.0	1.7
A05-537	141119	05-Jul-05	378.64	−8.197	58.7	2.2
A05-561	124377	28-Jul-05	374.95	−8.004	54.9	1.7
A05-560	124373	28-Jul-05	374.95	−8.004	59.2	1.7
A05-680	125570	07-Sep-05	373.02	−7.917	56.2	1.7
A05-681	125570	07-Sep-05	373.02	−7.917	59.7	1.7
A05-721	125592	27-Oct-05	378.91	−8.216	59.7	1.7
A05-722	125609	27-Oct-05	378.91	−8.216	61.4	1.7
A05-777	124383	03-Nov-05	378.48	−8.143	57.6	1.7
A05-778	124401	03-Nov-05	378.48	−8.143	59.5	1.7
A06-177	131546	25-Jan-06	384.43	−8.388	53.5	1.7
A06-230	131038	15-Feb-06	385.30	−8.445	53.1	1.7
A06-244	131502	17-Mar-06	386.10	−8.503	50.4	1.7
A06-248	131105	17-Mar-06	386.10	−8.503	51.2	1.7
A06-315	131123	21-Apr-06	386.41	−8.491	50.7	1.7
A06-317	141188	21-Apr-06	386.41	−8.491	56.6	2.2
A06-381	131085	22-May-06	387.10	−8.535	58.6	1.7
A06-412	131542	12-Jun-06	383.75	−8.357	56.0	1.7
A06-543	131519	17-Jul-06	381.26	−8.194	56.3	1.7
A06-592	131077	03-Aug-06	377.03	−7.996	57.3	1.7
A06-593	131053	13-Sep-06	376.65	−7.987	54.9	1.7
A06-632	131137	06-Oct-06	378.45	−8.061	56.3	1.7
A06-633	138036	06-Oct-06	378.45	−8.061	57.6	2.2
A06-641	131511	09-Nov-06	383.20	−8.274	56.0	1.7
A07-087	138130	11-Jan-07	386.06	−8.444	52.0	2.2
A07-128	141192	23-Feb-07	386.98	−8.461	51.4	2.2
A07-127	138101	23-Feb-07	386.98	−8.461	53.9	2.2
A07-198	138075	27-Mar-07	387.85	−8.50[a]	46.7	2.2
A07-330	138062	04-May-07	388.27	−8.50[a]	48.7	2.2
A07-404	138092	07-Jun-07	388.06	−8.50[a]	44.1	2.2
A07-572	138112	17-Jul-07	380.83	−8.20[a]	55.4	2.2
A07-581	138104	07-Aug-07	377.49	−8.00[a]	52.0	2.2
A07-599	138134	06-Sep-07	377.51	−8.00[a]	51.9	2.2
A08-055	141128	12-Oct-07	381.60	−8.10[a]	53.3	2.2
A08-061	141136	07-Dec-07	385.72	−8.30[a]	42.3	2.2

[a]Estimated $\delta^{13}C$ values, when direct measurements were not available.

[53] **Acknowledgments.** The air sampling and CO_2 extractions were supported by a grant from BP, by the National Science Foundation (NSF) under grant ATM-0632770, the U.S. Department of Energy (DOE) under grant DE-FG02-07ER64362 as well as by previous awards from NSF and DOE. This work was performed in part under the auspices of the U.S. Department of Energy by Lawrence Livermore National Laboratory under contract W-7405-Eng-48 and DE-AC52-07NA27344. Radiocarbon analyses were funded by grants from NOAA's Office of Global Programs (NA05OAR4311166) and LLNL's Directed Research and Development program (06-ERD-031) to T.P.G. H.D.G. received support from the UC Office of the President and a NASA ESS Fellowship. H.D.G. also thanks Nicolas Gruber for support and helpful discussions. Alane Bollenbacher conducted CO_2 and stable isotope analyses. We thank the anonymous reviewers and Jocelyn Turnbull for helpful comments, Ingeborg Levin for sharing recent $\Delta^{14}C$ data from Jungfraujoch and Christian Rödenbeck for assistance with the TM3 Model. This research was also presented in H.D. G.'s doctoral dissertation at the University of California, San Diego, USA, 2008.

References

Andres, R. J., G. Marland, I. Fung, and E. Matthews (1996), A 1° × 1° distribution of carbon dioxide emissions from fossil fuel consumption and cement manufacture, 1950–1990, *Global Biogeochem. Cycles*, *10*, 419–429.

Anzai, K., S. Keta, M. Kano, N. Ishihara, T. Moriyama, Y. Okamura, K. Ogaki, and K. Nodaa (2008), Radioactive effluent releases from Rokkasho Reprocessing plant 1. Gaseous effluent, technical report, Reprocess. Bus. Div., Japan Nuclear Fuel Limited, Rokkasho, Japan.

Baldwin, M. P., et al. (2001), The quasi-biennial oscillation, *Rev. Geophys.*, *39*(2), 179–230.

Canadell, J., et al. (2007), Contributions to accelerating atmospheric CO_2 growth from economic activity, carbon intensity, and efficiency of natural sinks, *Proc. Natl. Acad. Sci. U. S. A.*, *104*(47), 18,866–18,870.

Cantrell, C. A. (2008), Technical Note: Review of methods for linear least-squares fitting of data and application to atmospheric chemistry problems, *Atmos. Chem. Phys.*, *8*, 5477–5487.

Conil, S., and A. Hall (2006), Local regimes of atmospheric variability: A case study of Southern California, *J. Clim.*, *19*, 4308–4325.

Conway, T. J., and P. Tans (2004), Atmospheric carbon dioxide mixing ratios from the NOAA CMDL Carbon Cycle Cooperative Global Air Sampling Network (2004), in *Trends: A Compendium of Data on Global Change*, ftp://cdiac.ornl.gov/pub/ndp005/README_co2.html, Carbon Dioxide Inf. Anal. Cent., Oak Ridge Natl. Lab., U.S. Dep. of Energy, Oak Ridge, Tenn.

Cramer, W., et al. (2001), Global response of terrestrial ecosystem structure and function to CO_2 and climate change: Results from six dynamic global vegetation models, *Global Change Biol.*, *7*, 357–373.

Currie, K. I., G. Brailsford, S. Nichol, A. Gomez, R. Sparks, K. R. Lassey, and K. Riedel (2009), Tropospheric $^{14}CO_2$ at Wellington, New Zealand: The world's longest record, *Biogeochemistry*, *104*(1–3), 5–22, doi:10.1007/s10533-009-9352-6.

Dutta, K. (2002), Coherence of tropospheric $^{14}CO_2$ with El Niño/Southern Oscillation, *Geophys. Res. Lett.*, *29*(20), 1987, doi:10.1029/2002GL014753.

Enting, I. G. (1987), On the use of smoothing splines to filter CO_2 data, *J. Geophys. Res.*, *92*(9), 10,977–10,984.

Fallon, S. J., T. P. Guilderson, and T. A. Brown (2007), CAMS/LLNL ion source efficiency revisited, *Nucl. Inst. Phys. Res. B*, *259*, 106–110.

Friedli, H., H. Lötscher, H. Oeschger, U. Siegenthaler, and B. Stauffer (1986), Ice core record of $^{13}C/^{12}C$ ratio of atmospheric CO_2 in the past two centuries, *Nature*, *324*, 237–238.

Friedlingstein, P., et al. (2006), Climate-carbon cycle feedback analysis: Results from the C^{4}MIP model intercomparison, *J. Clim.*, *19*, 3337–3353.

Goudriaan, J. (1992), Biosphere structure, carbon sequestering potential and the atmospheric ^{14}C carbon record, *J. Exper. Bot.*, *43*(8), 1111–1119.

Graven, H. D. (2008), Advancing the use of radiocarbon in studies of global and regional carbon cycling with high precision measurements of ^{14}C in CO_2 from the Scripps CO_2 Program, Ph.D. thesis, Scripps Inst. of Oceanogr., Univ. of Calif., San Diego, La Jolla.

Graven, H. D., and N. Gruber (2011), Continental-scale enrichment of atmospheric $^{14}CO_2$ from the nuclear power industry: Potential impact on the estimation of fossil fuel-derived CO_2, *Atmos. Chem. Phys.*, *11*, 12,339–12,349, doi:10.5194/acp-11-12339-2011.

Graven, H. D., T. P. Guilderson, and R. F. Keeling (2007), Methods for high-precision ^{14}C AMS measurement of atmospheric CO_2 at LLNL, *Radiocarbon*, *49*, 349–356.

Graven, H. D., B. B. Stephens, T. P. Guilderson, T. L. Campos, D. S. Schimel, J. E. Campbell, and R. F. Keeling (2009), Vertical profiles

of biospheric and fossil fuel-derived CO_2 and fossil fuel CO_2:CO ratios from airborne measurements of $\Delta^{14}C$, CO_2 and CO above Colorado, USA, *Tellus, Ser. B*, *61*, 536–546.

Graven, H. D., T. P. Guilderson, and R. F. Keeling (2012), Observations of radiocarbon in CO_2 at seven global sampling sites in the Scripps flask network: Analysis of spatial gradients and seasonal cycles, *J. Geophys. Res.*, *117*, D02302, doi:10.1029/2011JD016535.

Guenther, P. R., A. F. Bollenbacher, C. D. Keeling, E. F. Stewart, and M. Wahlen (2001), Calibration methodology for the Scripps $^{13}C/^{12}C$ and $^{18}O/^{16}O$ stable isotope program, 1996–2000, report, 118 pp., Scripps Inst. of Oceanogr. Univ. of Calif., San Diego, La Jolla.

Hamilton, K., and S. M. Fan (2000), Effects of the stratospheric quasi-biennial oscillation on long-lived greenhouse gases in the troposphere, *J. Geophys. Res.*, *105*(D16), 20,581–20,588.

Hamme, R. C., and R. F. Keeling (2008), Ocean ventilation as a driver of interannual variability in atmospheric potential oxygen, *Tellus, Ser. B*, *60*(5), 706–717.

Hesshaimer, V., M. Heimann, and I. Levin (1994), Radiocarbon evidence for a smaller oceanic carbon dioxide sink than previously believed, *Nature*, *370*(6486), 201–203.

Houghton, R. (2008), Carbon flux to the atmosphere from land-use changes: 1850–2005, in *Trends: A Compendium of Data on Global Change*, http://cdiac.ornl.gov/trends/landuse/houghton/houghton.html, Carbon Dioxide Inf. Anal. Cent., Oak Ridge Natl. Lab., U.S. Dep. of Energy, Oak Ridge, Tenn.

Hsueh, D. Y., N. Y. Krakauer, J. T. Randerson, X. Xu, S. E. Trumbore, and J. R. Southon (2007), Regional patterns of radiocarbon and fossil fuel-derived CO_2 in surface air across North America, *Geophys. Res. Lett.*, *34*, L02816, doi:10.1029/2006GL027032.

Jöckel, P., M. G. Lawrence, and C. A. M. Brenninkmeijer (1999), Simulations of cosmogenic ^{14}CO using the three-dimensional atmospheric model MATCH: Effects of ^{14}C production distribution and the solar cycle, *J. Geophys. Res.*, *104*(D9), 11,733–11,743.

Kawabata, H., H. Narita, K. Harada, S. Tsunogai, and M. Kusakabe (2003), Air-sea gas transfer velocity in stormy winter estimated from radon deficiency, *J. Oceanogr.*, *59*(5), 651–661.

Keeling, C. D. (1979), The Suess effect: ^{13}Carbon-^{14}Carbon interrelations, *Environ. Int.*, *2*(4–6), 229–300.

Keeling, C. D., and S. C. Piper (2001), Exchanges of atmospheric CO_2 and $^{13}CO_2$ with the terrestrial biosphere and oceans from 1978 to 2000. IV. Critical overview, *SIO Ref. Ser. 01–09*, 23 pp., Scripps Inst. of Oceanogr., Univ. of Calif., San Diego, La Jolla.

Keeling, C. D., and T. P. Whorf (2005), Atmospheric CO_2 records from sites in the SIO air sampling network, in *Trends: A Compendium of Data on Global Change*, Carbon Dioxide Inf. Anal. Cent., Oak Ridge Natl. Lab., U.S. Dep. of Energy, Oak Ridge, Tenn., http://cdiac.ornl.gov/trends/co2/sio-keel.html.

Keeling, C. D., R. B. Bacastow, A. F. Carter, S. C. Piper, T. P. Whorf, M. Heimann, W. G. Mook, and H. Roeloffzen (1989), A three-dimensional model of atmospheric CO_2 transport based on observed winds: 1. Analysis of observational data, in *Aspects of Climate Variability in the Pacific and the Western Americas*, *Geophys. Monogr. Ser.*, vol. 55, edited by D. H. Peterson, pp. 165–235, AGU, Washington, D. C.

Keeling, C. D., P. R. Guenther, G. Emanuele, A. Bollenbacher, and D. J. Moss (2002), Scripps reference gas calibration system for carbon dioxide-in-nitrogen and carbon dioxide-in-air standards: Revision of 1999, a report prepared for the Global Environmental Monitoring Program of the World Meteorological Organization, 83 pp., World Meteorol. Org., Geneva.

Keeling, C. D., A. F. Bollenbacher, and T. P. Whorf (2005), Monthly atmospheric $^{13}C/^{12}C$ isotopic ratios for 10 SIO stations, in *Trends: A Compendium of Data on Global Change*, http://cdiac.esd.ornl.gov/trends/co2/iso-sio/iso-sio.html, Carbon Dioxide Inf. Anal. Cent., Oak Ridge Natl. Lab., U.S. Dep. of Energy, Oak Ridge, Tenn.

Keeling, C. D., S. C. Piper, T. P. Whorf, and R. F. Keeling (2011), Evolution of natural and anthropogenic fluxes of atmospheric CO_2 from 1957 to 2003, *Tellus, Ser. B*, *63*, 1–22.

Keeling, R. F., A. C. Manning, E. M. McEvoy, and S. R. Shertz (1998), Methods for measuring changes in atmospheric O_2 concentration and their application in southern hemisphere air, *J. Geophys. Res.*, *103*(D3), 3381–3397.

Key, R. M., et al. (2004), A global ocean carbon climatology: Results from Global Data Analysis Project (GLODAP), *Global Biogeochem. Cycles*, *18*, GB4031, doi:10.1029/2004GB002247.

Krakauer, N., J. T. Randerson, F. W. Primeau, N. Gruber, and D. Menemenlis (2006), Carbon isotope evidence for the latitudinal distribution and wind speed dependence of the air-sea gas transfer velocity, *Tellus, Ser. B*, *58*(5), 390–417.

Lal, D. (1992), Expected secular variation in the global terrestrial production rate of radiocarbon, in *The Last Deglaciation: Absolute and Radiocarbon Chronologies*, edited by E. Bard and W. S. Broecker, pp. 113–126, Springer, Berlin.

Lal, D., and Rama (1966), Characteristics of global tropospheric mixing based on man-made ^{14}C, ^{3}H, and ^{90}Sr, *J. Geophys. Res.*, *71*, 2865–2874.

Levin, I., and V. Hesshaimer (2000), Radiocarbon—A unique tracer of global carbon cycle dynamics, *Radiocarbon*, *42*(1), 69–80.

Levin, I., and B. Kromer (2004), The tropospheric $^{14}CO_2$ level in mid-latitudes of the Northern Hemisphere (1959–2003), *Radiocarbon*, *46*(3), 1261–1272.

Levin, I., and C. Rödenbeck (2008), Can the envisaged reductions of fossil fuel CO_2 emissions be detected by atmospheric observations?, *Naturwissenschaften*, *95*(3), 203–208.

Levin, I., B. Kromer, H. Schoch-Fischer, M. Bruns, M. Münnich, B. Berdau, J. C. Vogel, and K. O. Münnich (1985), 25 years of tropospheric ^{14}C observations in central Europe, *Radiocarbon*, *27*(1), 1–19.

Levin, I., J. Schuchard, B. Kromer, and K. O. Münnich (1989), The continental European Suess Effect, *Radiocarbon*, *31*(3), 431–440.

Levin, I., B. Kromer, M. Schmidt, and H. Sartorius (2003), A novel approach for independent budgeting of fossil fuel CO_2 over Europe by $^{14}CO_2$ observations, *Geophys. Res. Lett.*, *30*(23), 2194, doi:10.1029/2003GL018477.

Levin, I., B. Kromer, L. P. Steele, and L. W. Porter (2007), Continuous measurements of ^{14}C in atmospheric CO_2 at Cape Grim, 1997–2006, in *Baseline Atmospheric Program Australia 2005–2006*, pp. 57–59, Aust. Bur. of Meteorol., Melbourne, Victoria, Australia.

Levin, I., et al. (2010), Observations and modelling of the global distribution and long-term trend of atmospheric $^{14}CO_2$, *Tellus, Ser. B*, *62*, 26–46.

Lowe, D. C., and W. Allan (2002), A simple procedure for evaluating global cosmogenic ^{14}C production in the atmosphere using neutron monitor data, *Radiocarbon*, *44*(1), 149–157.

Manning, M. R., D. C. Lowe, W. H. Melhuish, R. J. Sparks, G. Wallace, C. A. M. Brenninkmeijer, and R. C. McGill (1990), The use of radiocarbon measurements in atmospheric studies, *Radiocarbon*, *32*(1), 37–58.

Manning, M. R., D. C. Lowe, R. C. Moss, G. E. Bodeker, G. Wallace, and W. Allan (2005), Short-term variations in the oxidizing power of the atmosphere, *Nature*, *436*, 1001–1004.

Marland, G., T. A. Boden, and R. J. Andres (2007), Global, regional, and national fossil fuel CO_2 emissions, in *Trends: A Compendium of Data on Global Change*, http://cdiac.ornl.gov/trends/emis/overview_2007.html, Carbon Dioxide Inf. Anal. Cent., Oak Ridge Natl. Lab., U.S. Dep. of Energy, Oak Ridge, Tenn.

Marland, G., T. A. Boden, and R. J. Andres (2008), Global, regional, and national fossil fuel CO_2 emissions (1751–2008), in *Trends: A Compendium of Data on Global Change*, http://cdiac.ornl.gov/trends/emis/overview_2008.html, Carbon Dioxide Inf. Anal. Cent., Oak Ridge Natl. Lab., U.S. Dep. of Energy, Oak Ridge, Tenn.

Marquis, M., and P. Tans (2008), Climate change: Carbon crucible, *Science*, *320*(5875), 460–461.

Masarie, K. A., and P. P. Tans (1995), Extension and integration of atmospheric carbon dioxide data into a globally consistent measurement record, *J. Geophys. Res.*, *100*(D6), 11,593–11,610.

Masarik, J., and J. Beer (1999), Simulation of particle fluxes and cosmogenic nuclide production in the Earth's atmosphere, *J. Geophys. Res.*, *104*(D10), 12,099–12,112.

Masarik, J., and J. Beer (2009), An updated simulation of particle fluxes and cosmogenic nuclide production in the Earth's atmosphere, *J. Geophys. Res.*, *114*, D11103, doi:10.1029/2008JD010557.

Meijer, H. A. J., H. M. Smid, E. Perez and M. G. Keizer (1996), Isotopic characterisation of anthropogenic CO_2 emissions using isotopic and radiocarbon analysis, *Phys. Chem. Earth*, *21*(5–6), 483–487.

Naegler, T., and I. Levin (2006), Closing the global radiocarbon budget 1945–2005, *J. Geophys. Res.*, *111*, D12311, doi:10.1029/2005JD006758.

Naegler, T., and I. Levin (2009), Biosphere-atmosphere gross carbon exchange flux and the $\delta^{13}CO_2$ and $\Delta^{14}CO_2$ disequilibria constrained by the biospheric excess radiocarbon inventory, *J. Geophys. Res.*, *114*, D17303, doi:10.1029/2008JD011116.

Naegler, T., P. Ciais, K. Rodgers, and I. Levin (2006), Excess radiocarbon constraints on air-sea gas exchange and the uptake of CO_2 by the oceans, *Geophys. Res. Lett.*, *33*, L11802, doi:10.1029/2005GL025408.

Nakada, A., T. Miyauchi, K. Akiyama, T. Momose, T. Kozawa, T. Yokota, and H. Ohtomo (2008), Radioactive airborne effluent discharged from Tokai reprocessing plant (1998–2007), technical report, Japan At. Energy Agency, Tokai-mura, Japan.

Neftel, A., H. Friedli, E. Moor, H. Lötscher, H. Oeschger, U. Siegenthaler, and B. Stauffer (1994), Historical CO_2 record from the Siple Station ice core, in *Trends: A Compendium of Data on Global Change*, http://

cdiac.ornl.gov/trends/co2/siple.html, Carbon Dioxide Inf. Anal. Cent., Oak Ridge Natl. Lab., U.S. Dep. of Energy, Oak Ridge, Tenn.

Nisbet, E. (2005), Emissions control needs atmospheric verification, *Nature*, *433*(7027), 683.

Nydal, R., and K. Lövseth (1965), Distribution of radiocarbon from nuclear tests, *Nature*, *206*(4988), 1029–1031.

Nydal, R., and K. Lövseth (1983), Tracing bomb ^{14}C in the atmosphere 1962–1980, *J. Geophys. Res.*, *88*(C6), 3621–3642.

Nydal, R., A. Brenkert, and T. Boden (1998), Carbon-14 measurements in surface water CO_2 from the Atlantic, Indian and Pacific Oceans, 1965–1994, *NDP-057A*, Carbon Dioxide Inf. Anal. Cent., Oak Ridge Natl. Lab., U.S. Dep. of Energy, Oak Ridge, Tenn.

O'Brien, K. (1979), Secular variations in the production of cosmogenic isotopes in the earth's atmosphere, *J. Geophys. Res.*, *84*(A2), 423–431.

Oeschger, H., U. Siegenthaler, U. Schotterer, and A. Gugelmann (1975), A box diffusion model to study carbon dioxide exchange in nature, *Tellus*, *27*, 168–192.

Proctor, I. D., J. R. Southon, M. L. Roberts, J. C. Davis, D. W. Heikkinen, T. L. Moore, J. L. Garibaldi, and T. A. Zimmerman (1990), The LLNL ion source—Past, present and future, *Nucl. Instrum. Meth. Phys. Res. B*, *52*(3–4), 334–337.

Rafter, T. A. (1955), ^{14}C variations in nature and the effect on radiocarbon dating, *N. Z. J. Sci. Technol., Sect. B*, *37*(1), 20–38.

Rafter, T. A., and G. J. Fergusson (1957), "Atom Bomb Effect"—Recent increase of Carbon-14 content of the atmosphere and biosphere, *Science*, *126*(3273), 557–558.

Randerson, J. T., I. G. Enting, E. A. G. Schuur, K. Caldeira, and I. Y. Fung (2002), Seasonal and latitudinal variability of troposphere $\Delta^{14}CO_2$: Post bomb contributions from fossil fuels, oceans, the stratosphere, and the terrestrial biosphere, *Global Biogeochem. Cycles*, *16*(4), 1112, doi:10.1029/2002GB001876.

Randerson, J. T., C. A. Masiello, C. J. Still, T. Rahn, H. Poorter, and C. B. Field (2006), Is carbon within the global terrestrial biosphere becoming more oxidized? Implications for trends in atmospheric O_2, *Global Change Biol.*, *12*(2), 260–271.

Riley, W. J., D. Y. Hsueh, J. T. Randerson, M. L. Fischer, J. G. Hatch, D. E. Pataki, W. Wang, and M. L. Goulden (2008), Where do fossil fuel carbon dioxide emissions from California go? An analysis based on radiocarbon observations and an atmospheric transport model, *J. Geophys. Res.*, *113*, G04002, doi:10.1029/2007JG000625.

Rozanski, K., I. Levin, J. Stock, and R. E. Guevara Falcon (1995), Atmospheric $^{14}CO_2$ variations in the equatorial region, *Radiocarbon*, *37*, 509–516.

Sabine, C. L., et al. (2004), The oceanic sink for anthropogenic CO_2, *Science*, *305*(5682), 367–371.

Schneider, M., and Y. Marignac (2008), Spent nuclear fuel reprocessing in France, *Res. Rep. 4*, Int. Panel on Fissile Mater., Princeton, N. J.

Siegenthaler, U. (1983), Uptake of excess CO_2 by an outcrop-diffusion model of the ocean, *J. Geophys. Res.*, *88*(C6), 3599–3608.

Siegenthaler, U., and H. Oeschger (1987), Biospheric CO_2 emissions during the past 200 years reconstructed by deconvolution of ice core data, *Tellus, Ser. B*, *39*, 140–154.

Stephens, B. B., R. F. Keeling, M. Heimann, K. D. Six, R. Murnana, and K. Caldeira (1998), Testing global ocean carbon cycle models using measurements of atmospheric O_2 and CO_2 concentration, *Global Biogeochem. Cycles*, *12*, 213–230.

Stuiver, M., and H. A. Polach (1977), Discussion: Reporting of ^{14}C data, *Radiocarbon*, *19*(3), 355–363.

Stuiver, M., and P. D. Quay (1981), Atmospheric ^{14}C changes resulting from fossil fuel CO_2 release and cosmic ray flux variability, *Earth Planet. Sci. Lett.*, *53*, 349–362.

Stuiver, M., P. J. Reimer, and T. F. Braziunas (1998), High-precision radiocarbon age calibration for terrestrial and marine samples, *Radiocarbon*, *40*(3), 1127–1151.

Suess, H. E. (1955), Radiocarbon concentration in modern wood, *Science*, *122*, 415–417.

Sweeney, C., E. Gloor, A. R. Jacobson, R. M. Key, G. McKinley, J. L. Sarmiento, and R. Wanninkhof (2007), Constraining global air-sea gas exchange for CO_2 with recent bomb ^{14}C measurements, *Global Biogeochem. Cycles*, *21*, GB2015, doi:10.1029/2006GB002784.

Tans, P. P., A. F. M. de Jong, and W. G. Mook (1979), Natural atmospheric ^{14}C variation and the Suess effect, *Nature*, *280*(5725), 826–828.

Trumbore, S. (2000), Age of soil organic matter and soil respiration: Radiocarbon constraints on belowground C dynamics, *Ecol. Appl.*, *10*(2), 399–411.

Turnbull, J. C., J. B. Miller, S. J. Lehman, P. P. Tans, R. J. Sparks, and J. Southon (2006), Comparison of $^{14}CO_2$, CO, and SF_6 as tracers for recently added CO_2 in the atmosphere and implications for biological CO_2 exchange, *Geophys. Res. Lett.*, *33*, L01817, doi:10.1029/2005GL024213.

Turnbull, J. C., S. J. Lehman, J. B. Miller, R. J. Sparks, J. Southon, and P. P. Tans (2007), A new high precision $^{14}CO_2$ time series for North American continental air, *J. Geophys. Res.*, *112*, D11310, doi:10.1029/2006JD008184.

Turnbull, J. C., et al. (2009a), Spatial distribution of $\Delta^{14}CO_2$ across Eurasia: Measurements from the TROICA-8 expedition, *Atmos. Chem. Phys.*, *9*, 175–187.

Turnbull, J., P. Rayner, J. B. Miller, T. Naegler, P. Ciais, and A. Cozic (2009b), On the use of $^{14}CO_2$ as a tracer for fossil fuel CO_2: Quantifying uncertainties using an atmospheric transport model, *J. Geophys. Res.*, *114*, D22302, doi:10.1029/2009JD012308.

Turnbull, J. C., et al. (2011), Assessment of fossil fuel carbon dioxide and other anthropogenic trace gas emissions from airborne measurements over Sacramento, California in spring 2009, *Atmos. Chem. Phys.*, *11*, 705–721, doi:10.5194/acp-11-705-2011.

UK Environmental Agency (2008), Radioactivity in food and the environment, 2007, *RIFE 13*, Rotherham, U. K.

United Nations Scientific Committee on the Effects of Atomic Radation (2000), Sources and effects of ionizing radiation, technical report, Vienna. [Available at http://www.unscear.org/.]

van der Laan, S., U. Karstens, R. E. M. Neubert, I. T. van der Laan-Luijkx, and H. A. J. Meijer (2010), Observation-based estimates of fossil fuel-derived CO_2 emissions in the Netherlands using $\Delta^{14}C$, CO and ^{222}Radon, *Tellus, Ser. B*, *62*(5), 389–402, doi:10.1111/j.1600-0889.2010.00493.x.

Wilks, D. S. (1995), *Statistical Methods in the Atmospheric Sciences: An Introduction*, Academic, San Diego, Calif.

H. D. Graven and R. F. Keeling, Scripps Institution of Oceanography, University of California, San Diego, 9500 Gilman Dr., La Jolla, CA 92093-0244, USA. (hgraven@ucsd.edu; rkeeling@ucsd.edu)

T. P. Guilderson, Center for Accelerator Mass Spectrometry, Lawrence Livermore National Laboratory L-397, 7000 East Ave., Livermore, CA 94550, USA. (tguilderson@llnl.gov)